Resilient Coastal Sites For Conservation

In Hawai'i

Analie Barnett and Mark G. Anderson

The Nature Conservancy

CENTER FOR RESILIENT CONSERVATION SCIENCE

January 31, 2022

Please cite as: Barnett, A. and Anderson, M.G. 2022. Resilient Coastal Sites for Conservation in Hawai'i. The Nature Conservancy, Center for Resilient Conservation Science.

View the interactive map, download the data, and read the report at: http://nature.org/HIcoast

Funding: This research was funded by grants from the Doris Duke Charitable Foundation. The results are intended to address the needs of organizations and decision makers grappling with pressing climate-related issues in coastal and marine environments.

Acknowledgements

This project represents the final piece in a twelve-year, 50 state, collaborative project led by The Nature Conservancy's Center for Resilient Conservation Science. Over the course of project, we engaged over 287 scientists through our geographic steering committees, and we acknowledge that the quality and usability of the results is due to their careful review of the concepts, methods, data sources, and mapped results.

We deviated from this model slightly for Hawaii in order to complete the work during a global pandemic. Instead of assembling a large steering committee we worked closely with our Nature Conservancy colleagues in the Hawaii program who provided a similarly high level of review and expertise. Our thanks to Dr. Sam Gon III, the Conservancy's Senior Scientist Cultural Advisor, and Stephanie Tom, the Conservation Information Manager. Sam is a wealth of information on the ecology of the state. He has been a part of the Conservancy for over 30 years, first as the Ecologist for the Hawaii Natural Heritage Program, then as Director of Science for the state, and now as Senior Scientist and Cultural Advisor. Stephanie seems to know everything about every Hawaii dataset. She has acquired or created maps, geospatial data, satellite images, aerial videos, LIDAR, multispectral images, historical maps, and crowdsourced information to show forest recovery, create reference maps, plot new access routes, map natural barriers to ungulates, and map weed invasions. Kudos again to both, we could not have completed this project without their thoughtful help, careful review, and interesting stories.

Table of Contents

Figures

Tables

CHAPTER

1

INTRODUCTION

Objective

We assessed the coastal region of six Hawaiian Islands and estimated the relative resilience or vulnerability of sites containing tidal marsh, tidal flats, and anchialine pools. We identified the sites most likely to continue to support biological diversity and ecological functions under rising sea levels up to 6.5 feet due to their ability to migrate upslope and adapt. The results are summarized in this report and available via the accompanying data package and web site.

Abstract

Coastal wetlands are critical to the productivity and diversity of marine ecosystems and to the human economies they support. Though small in area, Hawaii's estuarine wetlands have an outsize impact by providing habitat for a variety of plants and animals, including rare and endangered species; protection from storm waves and erosion; recreation and fishing opportunities; nutrient cycling; and preservation of historic and cultural values. Hawaiian estuarine wetlands are characterized by swamps, salt- and mudflats, unique anchialine pools, and historic fishponds. As sea levels rise, the Hawaiian Islands are particularly vulnerable and are already experiencing increased rates of inundation and record coastal flooding. With revised estimates of sea level rise in the range of six and a half feet to almost nine feet by 2100 (Sweet et al., 2017), many of these critical estuarine wetland habitats and their ecosystem services could be lost.

The characteristics of some coastal wetlands make them more likely to adapt to sea level rise and remain diverse and productive even as they adjust to climate-induced changes. In this project, we comprehensively mapped these characteristics and estimated the relative resilience of coastal sites on six Hawaiian Islands. In brief, we assessed coastal sites comprised respectively, of tidal marsh, tidal flats, and anchialine pools on the islands of Hawai'i, Kaua'i, Lana'i, Maui, Moloka'i, and O'ahu. For each site, we estimated the amount of migration space available under twenty sea-level rise scenarios. We quantified physical properties of the tidal marsh and tidal flat complexes, and the amount of development potentially blocking migration of these habitats upslope as sea levels increase. We used previously published and peer-reviewed datasets. Physical factors assessed were the size of the migration space, the

size of the existing tidal complex, and the amount of shared upland edge between the tidal complex and its migration space. The sole condition factor we evaluated was the percent of the existing marsh's upland edge that is developed.

We synthesized the above attributes by estimating a resilience score for each site. To calculate a resilience score, we combined the physical and condition scores for each site into a single value. Resilience scores were calculated for each of twenty sea-level rise scenarios (0.5 to 10 feet). Our final maps are based on the 6.5-foot scenario because this scenario reveals the sites with the greatest long-term potential for adaptive response, and this scenario is a worst-case, but plausible outcome by the end of the century. We made the results even more robust by slightly boosting the resilience score if the size of a site's migration space showed a statistically significant increase from the 0.5-ft. scenario to the 10-ft. scenario, suggesting that the size will continue to increase after 6.5 feet.

The scores are presented relative to other sites of the same type by island. That is, tidal marsh sites on Moloka'i are only compared to other tidal marsh sites on Moloka'i; they are not compared to tidal marsh sites on O'ahu or to unconsolidated shore sites on Moloka'i. Scores are presented in standardized normalized values (z-scores), which are units of standard deviations (SD) above or below the mean score of all sites of the same type on an island (see Appendix I for more details). For example, a z-score of "3" for a tidal marsh site on O'ahu indicates that the site scores three standard deviations higher than the average score across all of O'ahu's tidal marsh sites.

Study Area

The study area encompassed the intertidal region landward to the 10-foot elevation zone of six Hawaiian Islands: Hawai'i, Kaua'I, Lana'i, Maui, Moloka'i, and O'ahu. This study focuses on the ecological resilience of estuarine wetlands in this region to sea level rise (SLR). Due to the Hawaiian Islands' small size, topography, soils, and microclimates, the area of estuarine wetlands is small and the wetland types are different than those found on the US mainland. Based on 2010-2011 NOAA high resolution (~2.4 m resolution) land cover for the six islands in our study area, there are almost 4,000 acres of land classified as estuarine wetlands, including unconsolidated shore, or 1% of the land area across the six islands (Table 1.1, NOAA, 2020a).

Table 1.1. Estuarine wetland and unconsolidated shore acreage by Hawaiian Island (NOAA, 2020a).

	Acreage		
Island	**Estuarine Wetland**	**Unconsolidated Shore***	**Total**
Hawai’i	41	31	72
Kaua’i	111	317	428
Lana’i	0	108	108
Maui	0	402	402
Moloka’i	1,563	83	1646
O’ahu	797	431	1228

*Restricted to coastal zone

Estuarine wetlands on the Hawaiian Islands have formed over time as the islands have gradually subsided and sea level has risen relative to the land (Macdonald et al., 1970). They tend to occur in ground-water discharge zones. Types of estuarine wetlands on the Hawaiian Islands include emergent wetlands found along river mouths, and those located along the wet and windward shores of the major islands. The introduction of mangrove has led to the development of small forested estuarine wetlands on Oahu and Molokai. The Hawaiian Islands also feature a unique type of estuarine wetland called anchialine pools that form in collapsed lava tubes and have a belowground connection to the sea (Hill, 1996). Anchialine pools are small, usually around one acre, and are home to rare flora and fauna. While fishponds constructed by native Hawaiians are artificial, they are another type of estuarine wetland important for both cultural and biodiversity resources (Hill, 1996).

Coasts and estuaries are also of great importance to humans. Tremendous material and aesthetic resources associated with shorelines have attracted and sustained humans for thousands of years. Coastal ecosystems help support the economy by providing beautiful places to live, opportunities for tourism, commercial fishing, seafood processing, shipping harbors, and transportation routes. The malfunctioning of coastal ecosystems due to sea level rise, pollution, habitat destruction, hypoxia, harmful algal blooms, fishery collapses, and/or increased coastal erosion can have devastating social and financial impacts for coastal communities.

The pace of sea level rise in the region is growing with recent estimates citing an increase of one inch every four years, which threatens 70% of Hawaii’s beaches (State of Hawaii, 2022). The impacts of SLR are being felt across the Hawaiian Islands and are evident in widespread coastal erosion, more frequent high tide flooding (Sweet et al. 2018), and more inland flooding. On O’ahu, Maui, and K’auai, 25% of beaches have been lost to erosion (Ngu, 2020). Shoreline hardening in response to these impacts has only exacerbated the problems. As a result, Hawaii has been the first state in the US to declare a climate emergency.

Approach

In this one-year project, we quantified the resilience of 1,593 coastal sites by compiling and analyzing region-wide data on factors that influence a site's vulnerability or resilience to SLR. Physical and condition attributes were assessed and integrated into a spatially explicit dataset. Using these attributes, we evaluated each site's tidal habitats and estimated their ability to migrate landward in concert with rising seas based on the size, shape, condition, and context of their available migration space. The relative resilience of each site was determined by comparing it to other sites on the same island. We hope the resulting maps and datasets will provide local communities, policy makers, resource managers, and conservationists with clear and objective information for understanding the vulnerable and resilient areas of their coasts.

CHAPTER 2

BACKGROUND

As sea levels rise and intense storms become more frequent, the impacts are being felt by coastal communities and there is an urgent and growing interest in building community and ecological resilience. Cities and towns are being forced to reconsider how and where to invest in their coastal resources. These decisions affect millions of people because SLR can alter coastal-based economies, disrupt livelihoods, or overwhelm existing infrastructure. Since 2007, TNC has led the development of an online decision support tool, "*Coastal Resilience*" (http://coastalresilience.org/), to help communities address the effects of climate change and natural disasters. The aim of the web site is to help coastal communities increase their resilience to climate change by identifying nature-based or green infrastructure solutions that will enable them to effectively protect, restore, and sustainably manage their natural resources while also strengthening local capacity for climate adaptation.

The challenge of identifying the places where conservation is likely to succeed in sustaining diverse and productive ecosystems is the topic of this study. The tools and products arising from this study can be used in conjunction with the *Coastal Resilience* tool or independently, depending on the needs of the user. Although *coastalresilience.org* is focused on facilitating decisions about human communities and green infrastructure, it is predicated on the need for diverse and productive coastal habitats. The question of how we sustain diverse and productive habitats while facilitating their inevitable migration and adaptation, is the topic of this study.

NOAA has sponsored a website, Digital Coast (https://coast.noaa.gov/digitalcoast/) that is focused on helping communities across the US address coastal issues, and it has become one of the most-used resources in the coastal management community. The web mapping tool allows users to visualize community-level impacts from coastal flooding or sea level rise and maintains data related to water depth, connectivity, flood frequency, socio-economic vulnerability, wetland loss and migration, and mapping confidence. We adapted the latest marsh migration data in NOAA's Sea Level Rise Viewer tool (Marcy et al. 2011; NOAA, 2020b) as the basis of our migration space models.

Our approach to mapping site resilience focuses on the characteristics of the underlying geophysical stage rather than on the dynamics of the biotic systems. We assume that the biotic systems will change in concert with the changing climate, but that sites with certain enduring physical characteristics will have a larger capacity to support diversity, productivity, and ecological function into the future (Anderson et al. 2014). This approach has been called "conserving nature's stage," and is supported by current and historical evidence (Lawler et al. 2015; Beier et al. 2015; Gill et al. 2015; Anderson & Ferree, 2010). In the case of coastal sites, the elevation, landforms, and parent material that underlie a site and its surrounding lands can determine whether the site has space and options for adaptation.

We use the term "site resilience" to distinguish this approach from "ecosystem resilience" as the latter implies that an ecosystem is rebounding back to a previous state. Site resilience, in contrast, refers to the capacity of a physical site to maintain species diversity and ecological function even as the composition and proportion of habitats change in response to climate change. A resilient site is characterized as an area with enough options to sustain species and ecosystems in the face of stress and uncertainty. Such options, or characteristics that foster resilience, may include topographic and elevation diversity that provide a range of habitat types and microclimates, and space for adaptive movements with minimal barriers that restrict the movement of species or ecosystems. A site without such options would be considered vulnerable in the face of climate change.

Prior to this study, we developed methods for estimating the resilience of terrestrial sites (Anderson et al., 2014) by evaluating a site's landscape diversity (microclimates created by a site's topography, elevation gradients, and wetlands) and local connectedness (the degree to which the land cover is conducive to the movement of organisms and the flow of ecological processes). We mapped areas with higher microclimate diversity and local connectedness across a range of geophysical sites within large geographic regions (e.g., Eastern US, Great Plains, Great Lakes) to identify resilient sites across the US (http://maps.tnc.org/resilientland/). We excluded the coastal region of these geographies so we could undertake a separate assessment that considered sea level rise and focused on the potential for coastal marsh migration. The terrestrial study has been used successfully to inform conservation decisions and we hope that this counterpart study addressing the coastal region will be equally useful.

Our approach has similarities to other models that estimate the vulnerability of coastal regions to SLR, erosion, and inundation. In particular, the USGS Coastal Vulnerabilities Index (Thieler & Hammar-Klose, 1999), InVEST Coastal Vulnerability Model (Sharp et al., 2016), and the National Estuarine Research Reserve multi-metric approach (Raposa et al., 2016). Ecosystem vulnerability, in these studies is defined in the terminology of the Intergovernmental Panel on Climate Change (IPCC) as a combination of sensitivity and exposure. A primary difference between these vulnerability studies and this study is that other than SLR, we do not use factors that are dependent on climate (e.g., exposure, surge potential, community composition). Instead, we assume all sites have high exposure, high surge potential, and a changing composition, and we then identify the sites with characteristics that allow them to persist and support diversity even under the extreme scenarios. By running multiple SLR scenarios and scaling our results to the extreme 6.5-foot SLR scenario, we can identify the sites with more options for adaptation. In our model, a site is not considered more vulnerable if it *has more exposure to risk*, rather it is considered more vulnerable if it *has no options for adapting to, or accommodating, risk*.

CHAPTER 3

DEFINING & MAPPING COASTAL SITES

A coastal site was defined as an area of land regularly flooded by saline tidal waters and that contained tidal and estuarine habitats. Our site definition encompassed the landforms, soils, and tidal inundation zones that define the boundary and regulate local processes. These physical features set the stage for a mix of biotic and abiotic habitats including salt marsh, tidal flats, and anchialine pools that may move or expand with changes in climate. We mapped each site individually, and our analysis centered on measuring the characteristics and processes that influence its ability to accommodate sea level rise (SLR) by migrating inland and adapting to new conditions. We evaluated tidal complexes and anchialine pools as well as their potential migration space. Below we discuss the methods we used to map each type of coastal site.

Tidal Complex

We used the term "tidal complex" to refer to a set of interconnected tidal and estuarine habitats that were spatially grouped into a contiguous area. The habitats included:

Tidal marsh: Intertidal wetlands of low energy environments that form expansive meadows or narrow shoreline fringes with salt-tolerant vegetation (i.e., salt marsh). Tidal marshes are one of the most productive ecosystems in the world, producing up to 20 tons of biomass per acre and providing shoreline stabilization, nutrient cycling, and critical wildlife habitat for many species of plants, invertebrates, mammals, and birds. Salt marshes also provide breeding, refuge, nursery, and forage habitats for marine fauna.

Brackish marsh: Brackish marshes are transitional between freshwater and salt marsh, and form along the upland edge of salt marshes where freshwater runoff or groundwater dilutes the salinity of the marsh surface. Dominated by bulrushes and sedges, the species vary depending on local hydrology and salinity levels.

Tidal flat: Non-vegetated sand and mud flats provide habitat for a variety of invertebrate, fish, and algal species. At low tide, many shorebird species, including the endangered Hawaiian stilt, use them for grazing and foraging.

Mapping Tidal Complexes

To identify and map tidal complexes for the six Hawaiian Islands of Hawai'i, Kaua'i, Lana'i, Maui, Moloka'i, and O'ahu, we used NOAA's 2010 C-CAP high resolution (~2.4-m) land cover data (NOAA, 2020a), which was also used in NOAA's Sea Level Rise Viewer marsh migration dataset (NOAA, 2020b). We selected all pixels coded as unconsolidated shore or one of three estuarine wetland types: forested, scrub/shrub, or emergent (Figure 3.1).

As several of the islands only had unconsolidated shore habitat or had large expanses of unconsolidated shore habitat without any estuarine tidal habitat, we created two types of tidal complex units: 1) tidal marsh, and 2) unconsolidated shore (Figure 3.1). Tidal marsh units had to contain mostly estuarine marsh habitat while unconsolidated shore units consisted entirely of tidal flat habitat as mapped by NOAA's C-CAP land cover datasets. Units that contained an intertwined mix of both marsh and flats (i.e., a few sites on Hawaii island) were assigned to tidal marsh. All grouped units were then converted to discrete polygons, assigned unique IDs, and the acreage and perimeter of each polygon was calculated. Upon review of the resultant complexes, we discovered some unconsolidated shore units that were located too far inland to be tidal, and we manually removed all these non-tidal occurrences.

We experimented with different ways to aggregate cells into discrete tidal complex units based on adjacencies and distances. No single approach worked perfectly as some distances resulted in units that seemed too big while others seemed too small, and the literature is sparse on distance thresholds for what constitutes an ecologically functioning tidal wetland complex. Based on review of different groupings and on input from TNC's Hawai'i chapter science staff, we chose to group pixels of estuarine habitat or unconsolidated shore that were connected along a common edge or shared a corner diagonally (i.e., eight nearest neighbors). This had the effect of aggregating cells that touched one another into a single unit that we called a "tidal complex" (Figure 3.1).

Figure 3.1. Tidal complexes. The map shows examples of an unconsolidated shore complex and tidal marsh complexes for the island of O'ahu, with the NOAA 2010 C-CAP land cover dataset from which these units were derived. Migration space (defined in following section) for sea level rise scenarios from 0.5 to 10 feet is shown in shades of orange.

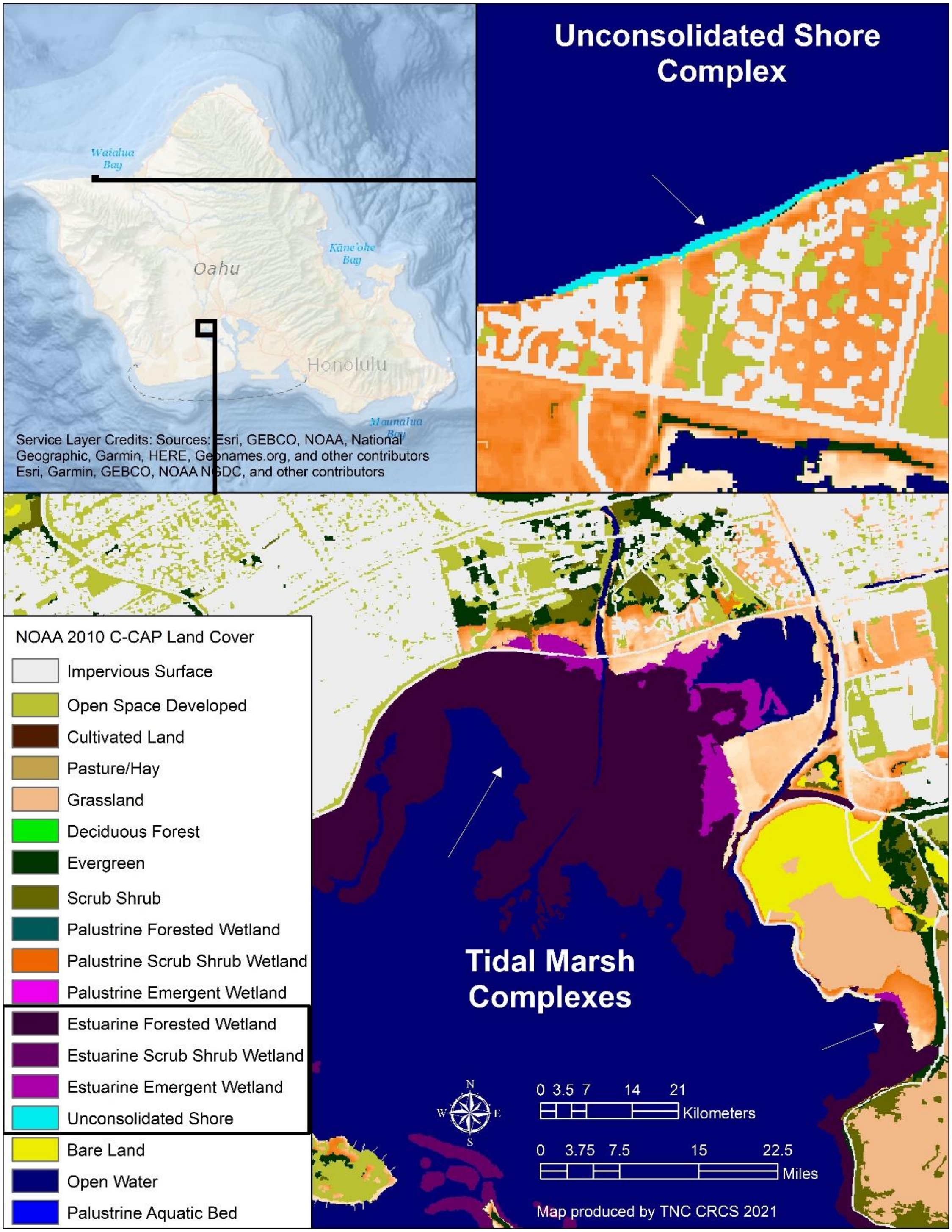

Anchialine Pools

Anchialine pools are enclosed brackish waterbodies near the ocean that occur in young volcanic and basalt substrates and have indirect, below-ground connections to the ocean. These coastal habitats are only found in the coastal tropics and subtropics and harbor unique and largely understudied biodiversity adapted to a range of salinity levels, including algae, shrimps, prawns, amphipods, and some fish species. Hawaiian anchialine pools are known to support at least seven rare aquatic species, two endangered waterbirds (Hawaiian Stilt and Hawaiian Coot), and provide stopover habitat for migratory waterfowl. Anchialine pools have been identified on five Hawaiian Islands, Hawai'I, Maui, Moloka'I, O'ahu, and Kaho'olawe, with the highest number found on Hawai'i. The invertebrate and algal diversity of some Hawaiian anchialine pools is thought to be the highest of anchialine pools in the Indo-Pacific and possibly globally.

To map Hawaiian anchialine pools, we obtained point locations of pools from The Nature Conservancy Hawai'i (Ecoregional Planning Team, 2006). As the spatial extent of each pool was unavailable, we buffered each point by 100 meters in a GIS and then removed any pixels of unsuitable land cover (e.g., developed) as shown in Figure 3.2. The one pool mapped on Moloka'i was located beyond our highest sea level rise scenario range of 10 feet and was not included in our analysis.

Figure 3.2. Anchialine pools. This map shows anchialine pools on Hawai'i. The bottom left panel shows a 100-m buffer around two anchialine pools with the 2010 NOAA C-CAP land cover. Gaps in the buffer of the top pool reflect the removal of unsuitable land cover, open water in this case. The bottom right panel overlays the anchialine pools with migration space delineated for SLR scenarios from 0.5 to 10 feet.

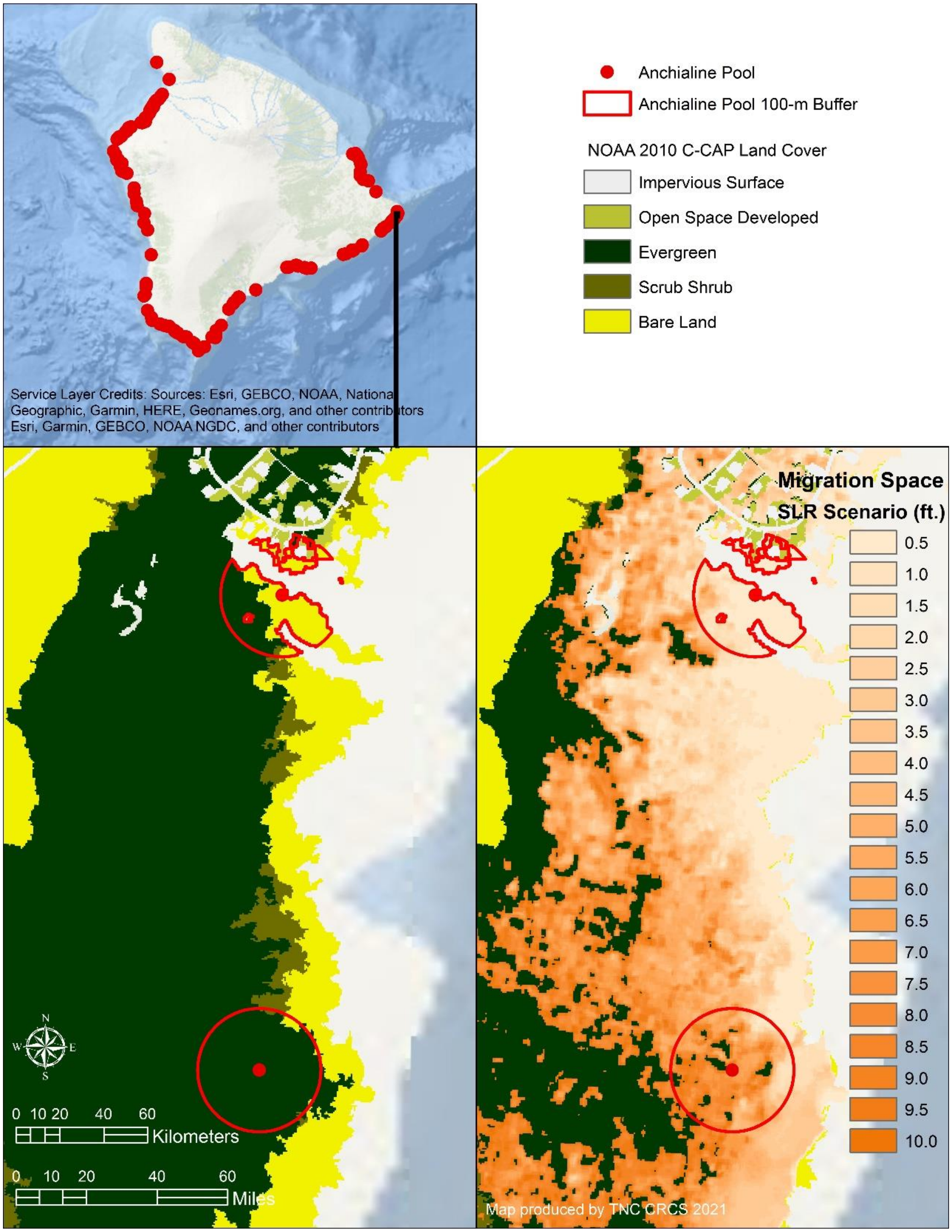

Migration Space

Migration space is defined as the area of low-lying land adjacent to the tidal complex that is potentially suitable for supporting tidal habitats in the future and into which the current habitats could migrate in response to rising sea levels. For example, as sea levels rose over the last century, Maryland's Blackwater National Wildlife Refuge gained 2,949 acres of new salt marsh at the existing marsh's upland edge (i.e., the migration space, Lerner et al. 2013). The concept of migration space appears in many coastal resilience studies where it has been variously called "accommodation space," "future marsh," "marsh migration opportunity areas," "migration pathways," "potential marsh zone," or "marsh migration opportunity areas" (Schuerch et al., 2018; C. Chaffee, pers. comm., 2017; K. Lucey, pers. comm., 2017; Maine Natural Areas Program, 2016). The transition process works like this: tidal marshes exist in a narrow zone between the mean high tide and the mean high-water line. As the tide rises, existing marshes become increasingly inundated, creating unsuitable conditions for vegetation growth and converting the marsh to unconsolidated substrate or open water. Meanwhile, new land suitable for habitat development may become available in the immediately adjacent lowlands as they start receiving regular tidal inundation. If conditions are right, the marsh may be able to migrate onto this land (Figure 3.3).

Sites vary widely in the amount and suitability of migration space they provide. This is determined by the physical structure of the site and the intactness of processes that facilitate migration. A marsh hemmed in by rocky cliffs will eventually convert to open water, whereas a marsh bordered by low lying wetlands with ample migration space and a sufficient sediment supply will have the option of moving inland.

As existing tidal marshes degrade or disappear, the amount of available high-quality migration space becomes an indicator of a site's potential to support estuarine habitats in the future. The physical size and shape of a site's migration space is dependent on the elevation, slope, and substrate of the adjacent land. The condition of the migration space also varies substantially among sites depending on the anthropogenic context. For some tidal complexes, the migration space contains roads, houses, and other forms of hardened structures that resist conversion to tidal habitats, while the migration space of other complexes consists of intact and connected freshwater wetlands that could convert to tidal habitats.

Figure 3.3. Migration space. Diagram illustrating how current tidal marsh is expected to move into its migration space, while the existing marsh is mostly lost to inundation. The image on the right shows the current marsh and migration space (orange) of tidal marshes located on the East End of Moloka'i, south of Kaluaaha Church.

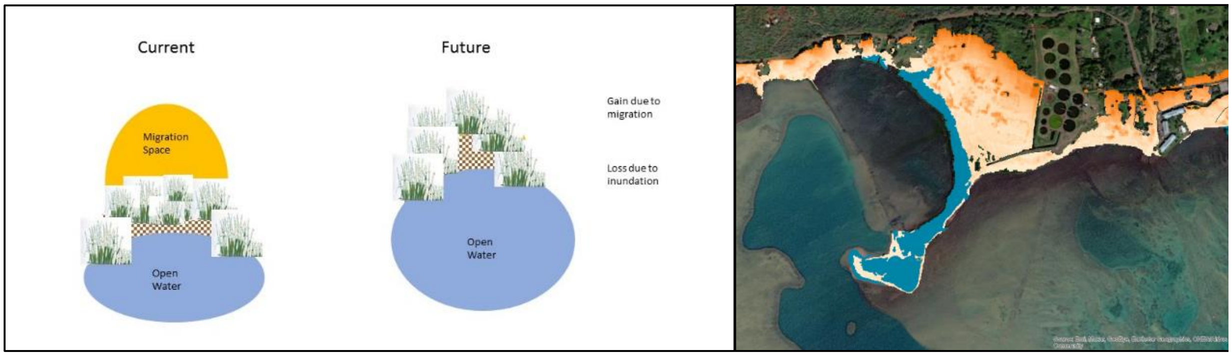

For the tidal complex units, our aim was to characterize each site's migration space and estimate its capacity to support a diverse coastal habitat in the future. Towards this end, we measured the amount of migration space associated with each marsh, and unconsolidated shore complex and how much of their upland boundary was shared with migration space. We assumed that most migration space will support some combination of salt marsh, brackish marsh, and tidal flat in the future, but we did not predict the future composition. Accurate predictions concerning the abundance and spatial arrangement of future tidal habitats are notoriously difficult to make because habitat transitions are often non-linear and facilitated by pulses of disturbance and internal competition among species. For instance, in response to a small 1.4 mm increase in the rate of SLR, the landward migration of low marsh cordgrass in some New York marshes appears to be displacing high marsh much more quickly than expected (Donnelly & Bertness, 2001). Our assumption was simply that a tidal complex with a large amount of high quality migration space will have more options for adaptation, and will be more resilient, than a tidal complex with a small amount of degraded and inaccessible migration space. For anchialine pools, we assumed that as pockets of open water develop in the migration space of anchialine pools, the pools and their biota will migrate to these areas. Without the extent of the anchialine pools, we did not assess how much of their upland boundary was shared with migration space.

Mapping Migration Space

Based on previous projects in the South Atlantic (Anderson & Barnett, 2019a) and the Gulf of Mexico (Anderson & Barnett, 2019b), we opted to use NOAA's SLR Viewer Marsh Migration datasets (NOAA, 2020b) which were developed to map potential impacts to marsh habitats from sea level rise. Datasets were available for the six

Hawaiian Islands and were developed using a modified bathtub inundation approach that considers local and regional tidal variability for multiple SLR scenarios. Our approach here was to start with the latest NOAA SLR model marsh migration data, convert it into a model of migration space, and then assess the amount of migration space potentially available for each coastal site.

The NOAA data does not map migration space per se, but instead predicts the distribution of future habitat types based on SLR scenarios and tidal class thresholds. To convert the results to migration space, we combined the area of three predicted habitat classes: brackish marsh, tidal marsh, and tidal flat into a single spatial extent. This simplified the individual habitat models into a single area of delineated migration space and eliminated error in habitat class predictions by focusing only on their combined spatial extent.

To delineate migration space for the full project area, we obtained the latest SLR Viewer marsh migration data from NOAA (N. Herold, pers. comm., 2020), with no accretion rate, for six Hawaiian Islands, Hawai'i, Kaua'i, Lana'i, Maui, Moloka'i, and O'ahu. We chose not to use any of the three SLR Viewer accretion rates because they were constants applied across each island while actual accretion is very location specific. For each island, we combined all SLR scenarios (0.5 to 10 feet by 0.5-ft. increments) with the baseline scenario to identify pixels that changed from current baseline. We only selected cells that transitioned to tidal habitats (unconsolidated shoreline, salt marsh, and transitional/brackish marsh) and not to open water or upland habitat. We projected all results to NAD83 Albers UTM Zone 4.

For each SLR scenario, the resultant migration space was spatially grouped into contiguous regions using an eight-neighbor rule that defined connected cells as those immediately to the right, left, above, or diagonal to each other. The region-grouped grid was converted to a polygon, and the SLR scenario represented by each migration space footprint was assigned to each polygon. In addition, for each SLR scenario greater than 0.5 feet, all lower SLR scenarios were merged with the highest SLR scenario on top. For example, the migration space for the 6.5-ft. SLR scenario was merged on top the migration space for all SLR scenarios less than 6.5 (i.e., 0.5 to 6.0-ft.). That grid was then spatially grouped into contiguous regions using an eight-neighbor rule, converted to polygon, and dissolved on unique region group ID. Finally, those migration space scenario polygons that intersected any of the tidal complexes or buffered anchialine pools were selected for use in this study.

A single migration space polygon could be adjacent to and accessible to more than one tidal complex unit, so each migration space polygon was linked to its respective tidal complex unit(s) with a unique ID by restructuring and aggregating the output from a one-to-many spatial join in ArcGIS. This linkage enabled the calculation of attributes for each tidal complex and each migration space such as total acreage, total number of units, and the percent of the tidal complex perimeter that was immediately adjacent to migration space.

Migration Space Scenarios

The amount of migration space available to a tidal complex or anchialine pool is a function of the surrounding elevation and topography, combined with the amount of expected sea level rise. Initial estimates of global sea level rise over the next century suggested a range from 1.6 to 4.6 feet (Rahmstorf et al., 2007; IPCC, 2013) and have recently increased by up to three additional feet based on the volatility of the Antarctic ice sheet (DeConto & Pollard, 2016). In the US, an interagency team led by NOAA recently revised the lower and upper bounds of their global and regional sea level rise scenarios for 2100 based on the latest peer-reviewed research on global mean sea level rise that considers the possibility of rapid ice melt in Greenland and Antarctica (Sweet et al., 2017). The estimates have been increased from 0.65– 6.5 ft. up to 1.0 to 8.2 ft. (0.2 - 2.0 m up to 0.3 - 2.5 m). The report also found that along all US coasts except Alaska, relative sea level is expected to be greater than the global average under several of the scenarios.

To map a range of possible migration space amounts we estimated its extent with respect to twenty SLR scenarios: 0.5′ to 10′ (Figure 3.4). Results for all scenarios are available to users of this project (see accompanying spatial datasets). However, we scaled our results to the 6.5-ft. scenario because we wanted to identify sites that were robust to more extreme events and a 6.5-ft. scenario has been recommended as an appropriate for planning purposes.

In the results presented here, tidal complex sites with increasing migration space over all scenarios scored higher than sites whose migration space declined with increasing inundation. We examined the trend of the migration space size from the 0.5 to 10-foot scenario to identify sites where the migration space was continuing to increase in size (Figure 3.5). This was done by fitting a regression line to the size of the new migration space across all SLR scenarios. Sites where the regression showed a significant trend ($p \leq 0.05$) were scored as increasing, decreasing, or no change depending on the trend sign (positive or negative). Sites that had a significant positive trend in migration space size received a small bonus of 0.5 SD to their final resilience score.

Figure 3.4. Migration space scenarios. This map shows the migration space under several SLR scenarios from 0.5 to 10-ft. for tidal marsh complexes in Kaloko-Honokōhau National Historical Park in the Kona District of Hawai'i. The amount of migration space accumulates for each scenario, but at this site, most migration space is gained during the middle SLR scenarios (4.0 ft. to 6.0 ft.).

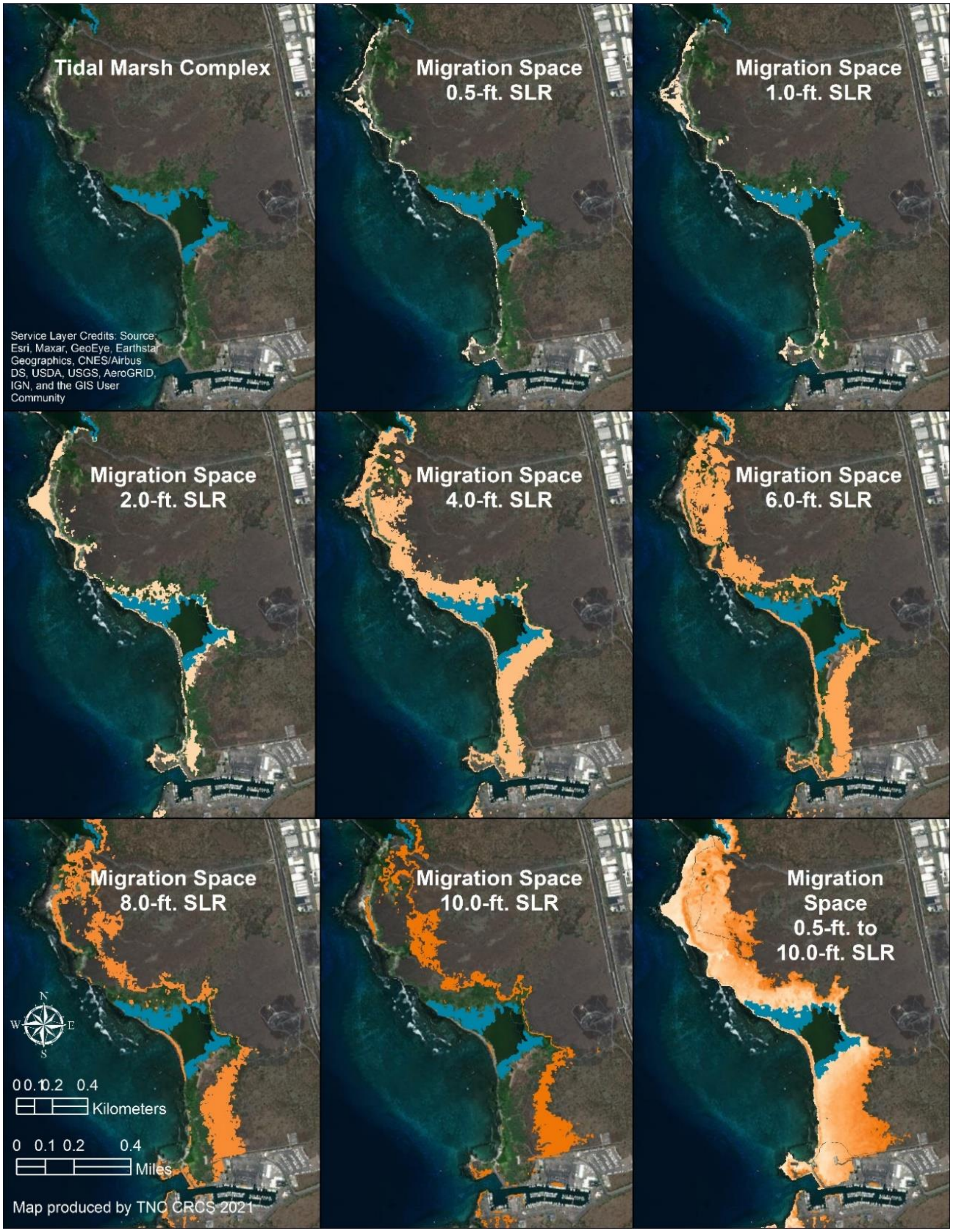

Figure 3.5. Migration space trend. The diagram shows the 0.5 to 10-foot SLR scenarios for two sites. Site A has moderate migration space under the 0.5-foot scenario but its migration space increases over later scenarios. The site on the right has the same size migration space for the 0.5-foot scenario, but the migration space decreases with each subsequent scenario. The chart shows how the trend would appear in the regression analysis.

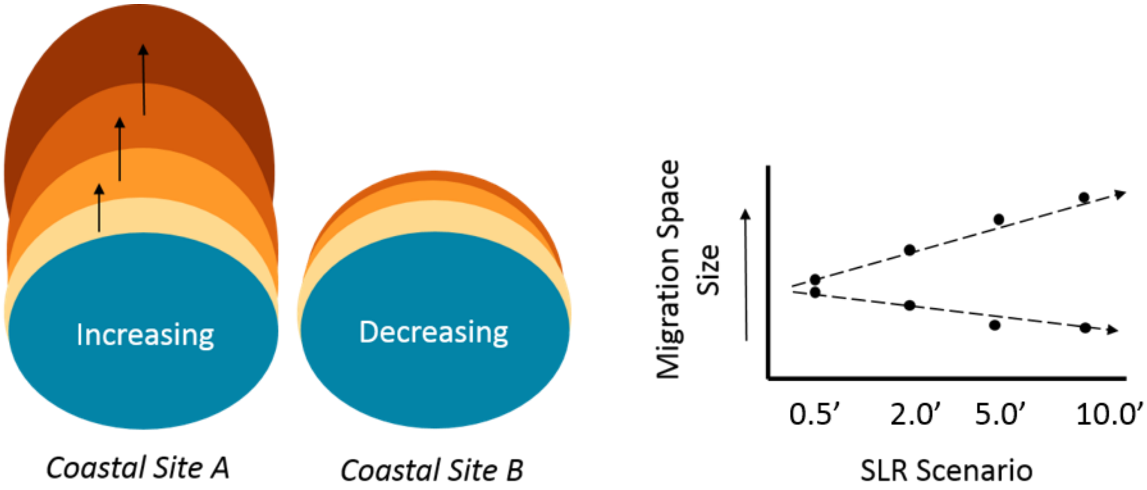

CHAPTER

4

ESTIMATING SITE RESILIENCE

This section describes the concepts and methods we used to estimate the resilience of a coastal site. We define "site resilience" as the ability of a site to support biological diversity and ecological functions even as it changes in response to climate change and SLR (Anderson et al., 2016). We expect coastal sites to change dramatically over the next century with new tidal habitats forming and migrating into the adjacent low lands where suitable migration space is available, and some existing marsh, tidal flats, and anchialine pools converting to open water. Identifying places where conservation can succeed, and restoration actions to help sites adapt to change, are necessary steps in sustaining the diversity and functions of coastal habitats.

In this study, we estimate a tidal complex's resilience to SLR based primarily on the size and accessibility of its migration space. Physical characteristics change slowly and are expected to endure under both current and future climates, making them a useful template for conservation planning. By evaluating the physical and condition characteristics of each site, we can identify the sites with relatively more options for migration and rearrangement. A site with extensive high-quality migration space that is not cut off by development offers more chances for rearrangement and adaptation than a site with little migration space flanked by roads and development. We can reasonably call the first site more "resilient" and the second site more "vulnerable" based on the measurable differences in options for adaptation. Admittedly, we do not know exactly how natural changes will play out at either site, because predicting the precise amount and spatial arrangement of each individual component in the future depends on thousands of specific climatic, hydrologic, and biotic changes, and there are large uncertainties about each of these. To evaluate the potential resilience of anchialine pools to different SLR scenarios, we could only use the size of each pool's migration space as the extent of each pool was not available.

For each attribute, we clarified the mechanism by which it increased options for adaptation, and we tested whether we could consistently measure the attribute across the study area with the precision needed to make realistic judgment about the site. We narrowed the attribute list to three physical characteristics and one condition attribute that have a quantifiable effect on the resilience of a tidal complex and could be adequately mapped at a regional scale (Box 4.1). We present the four attributes in the next section, and reiterate that we only measured the amount of migration space for anchialine pools. While we were unable to assess water quality, flow alteration, and sediment inputs for tidal complexes and anchialine pools, these are additional attributes important for managers to consider when developing management, restoration, and conservation plans to accommodate sea level rise at individual sites.

Box 4.1. Physical and condition attributes to assess resilience of coastal sites.
Condition attributes are shown in italics.

Tidal Complex	**Anchialine Pool**
Physical Attributes • Amount of migration space • Shared upland edge with migration space (%) • Size of current tidal complex Condition Attributes • *Undeveloped upland marsh edge (%)*	Physical Attributes • Amount of migration space

Tidal Complex and Migration Space

This section focuses on identifying and mapping characteristics of the tidal complex and its migration space that increase a site's ability to adapt to SLR. Characteristics of the migration space are particularly critical to resilience because it represents the future distribution of the tidal complex, whereas characteristics of the current tidal complex are less influential because under most SLR scenarios the current complexes are unstable and expected to degrade or convert entirely to open water. Because the factors are unequal in their degree of influence, we used a weighting scheme to give more weight to factors hypothesized to have a large influence on site resilience and less weight to factors likely to have less influence, when we combined factors into a single index (Box 4.2 and Figure 4.1).

Box 4.2. Tidal complex and migration space attributes and data sources.

Physical Characteristics

Amount of Migration Space (Weight = 5): A large migration space is an essential condition for a large tidal complex in the future that supports robust species populations, allows for ecological processes, and is less susceptible to degradation. We both measured this quantitatively and applied a threshold to ensure a minimum size. Data source: NOAA SLR Viewer Marsh Migration data

Shared Upland Edge between Migration Space and Tidal Complex (Weight = 2): The migration of tidal habitats into the adjacent lowlands is facilitated by migration space directly adjacent to the upland edge of existing marshland. Data sources: NOAA 2010 C-CAP, NOAA SLR Viewer Marsh Migration data

Size of Existing Tidal Complex (Weight = 2): The size of the tidal complex is likely to influence its ability to migrate as large complexes provide large sources of biotic material. Data source: NOAA 2010 C-CAP

Condition Characteristics

Developed Upland Edge: Tidal complexes with development and roads along their upland edge have less access to their migration space and a lower likelihood of upland migration. Data sources: NOAA 2010 C-CAP

Data Source References: **NOAA SLR Viewer Marsh Migration Data** (Herold, 2020; NOAA, 2020b), **NOAA C-CAP 2010** (NOAA, 2020a)

Figure 4.1. Tidal complex and migration space characteristics that increase resilience. Characteristics of a resilient site are shown on the left and contrasted with a vulnerable site on the right. Factors with a strong influence are listed in bold and located above factors with less influence.

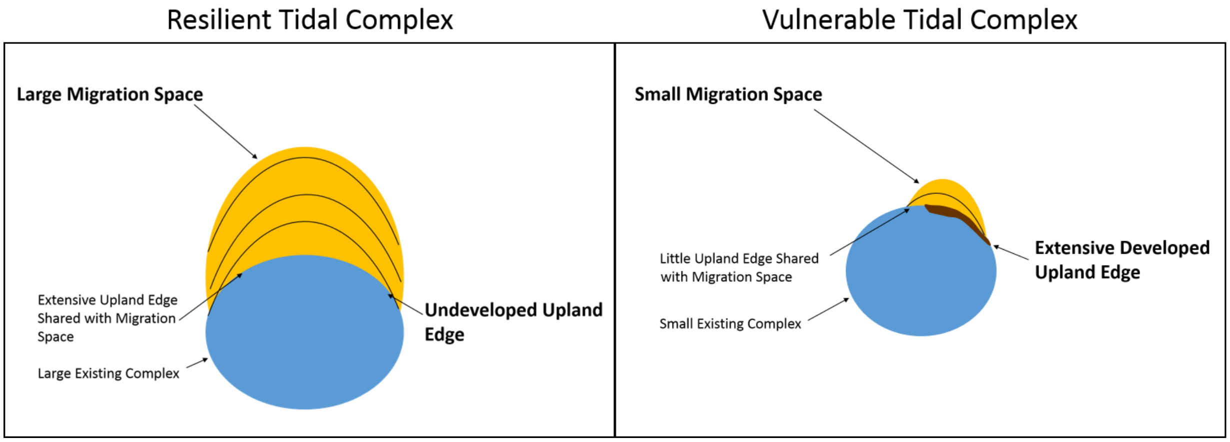

Physical Characteristics

The physical characteristics of a site determine if suitable land is available to support the migration of tidal habitats, and the probability that colonizers will be able to access and utilize the migration space. These factors focus on the size and configuration of the migration space. For all the physical characteristics, we assumed that a large range increased resilience because variation and flexibility increase the options for adaptation. For example, a large migration space offers more possibilities for sustaining diversity than a small migration space.

The physical attributes described below are arranged in order of influence. For each, we first describe how the attribute contributes to the site's resilience and then we explain the data sources and methods we used to map the attribute. The attributes were ordered with respect to their direct importance to site resilience, and then weighted on a numeric scale from 1 to 5 to reflect their influence, with 5 indicating the greatest influence. The numeric weights were used as a multiplier when combining factors to give more weight to factors with more influence: 5 (very high), 4 (high), 3 (moderate), 2 (low) and 1 (very low). The numeric weight is listed in parentheses after each attribute.

Physical Characteristics of the Migration Space

SIZE OF MIGRATION SPACE (WEIGHT = 5): A large migration space is an essential condition for a large tidal complex in the future, although we don't know how closely the space and the future size will correlate. Large areas of tidal habitat are more resilient because they sustain demographic and ecological processes that inherently require space within which to operate and support robust populations of keystone species such as saltmarsh grasses. Large marshes store more carbon, provide more storm buffer and are less susceptible to degradation from stochastic events, and they are also more likely to host rare species. Tidal complexes with small migration spaces are vulnerable if inundation levels reach the expected 2 to 6.5 feet, because existing tidal marshes will be stressed for oxygen and will likely degrade or disappear.

The relationship between a tidal complex and its migration space is complicated. A single tidal complex may have many non-contiguous regions of associated migration space and they may vary in size. Our estimate of total size is defined as the sum of all migration space units adjacent to the tidal complex (Figure 4.2). Additionally, estimates of migration space vary depending on the SLR scenario, and at higher scenarios, some portions may be inundated. Thus, total size for any scenario is based on the total of previous scenarios minus the amount converted to open water.

For anchialine pools, we took an additional step of identifying pools that were unlikely to be impacted by a sea level rise up to 10-feet. To do this, we ran a spatial overlay analysis between the inundation footprint for each SLR scenario and the buffered anchialine pools. We calculated the percent of each buffered pool likely to be remaining for each of the twenty SLR scenarios. We retained pools that showed a decreasing amount of area up to the 10-foot scenario. Specifically, we selected all pools with less than 95% of their area remaining for the 6.5-foot scenario and less than 90% of their area remaining for the 10-foot scenario. This reduced the total number of pools assessed in our analysis from 172 to 107 pools. We assume the pools that were not examined will be resilient well into the future as they are unlikely to be impacted by the most extreme 10-foot SLR scenario.

Figure 4.2. Tidal complex and migration space association. The diagram shows three different types of relationships that can exist between existing tidal complexes (blue) and migration space (orange). In the far-left diagram, the relationship between existing marsh and migration space is almost one-to-one. In the middle figure, some small complexes might unite under one migration space (one to many). The far right diagram illustrates how the current marsh will likely disassociate into many smaller marshes (many to one).

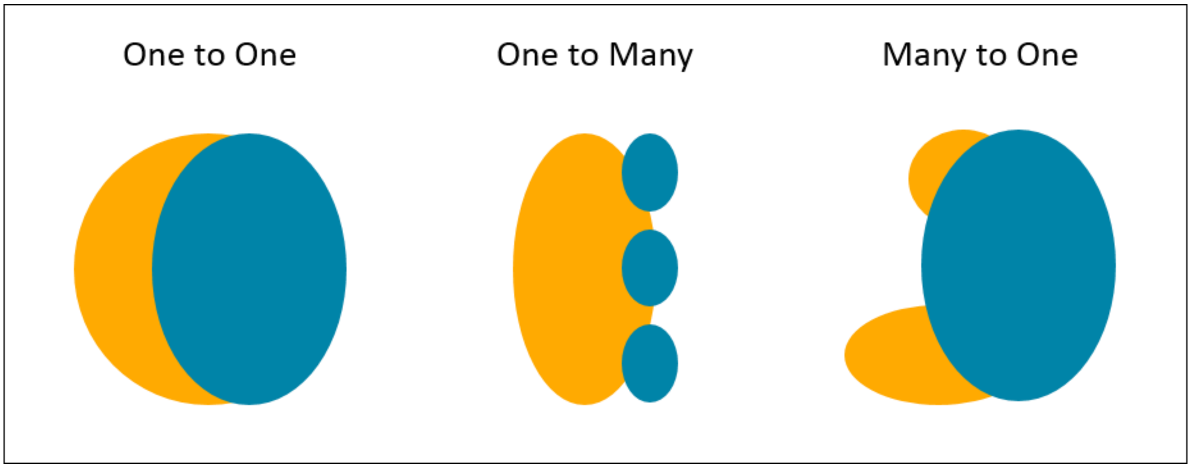

<u>SHARED UPLAND EDGE (WEIGHT = 2):</u> The migration of existing tidal habitats into the adjacent lowlands is facilitated by having migration space directly adjacent to the existing habitats. Having a high proportion of a tidal complex's upland edge shared with its migration space helps ensure that all regions of the tidal complex and all types of habitat have direct access to the migration space (Figure 4.3 A). It was not uncommon to have a relatively large patch of migration space touch only a small part of the existing complex, especially if the migration space was associated with a small river inlet. In these cases, migration could be hampered as not all the existing complex has easy access to the migration space (Figure 4.3 B).

To map the shared upland edge, we first identified the upland edge of each tidal complex in a GIS by removing all seaward edges based on an ocean/water grid derived from NOAA's 2010 C-CAP land cover grids for each island. The resulting tidal complex upland edge was then spatially intersected with the migration space units, and the output was set to a polyline. We calculated the length of the polyline output, the shared upland edge, from the intersection analysis. Lastly, for each complex, we divided the shared upland edge by the total upland edge length to calculate the percent of upland edge shared with migration space. While the tidal complexes did not change with SLR scenario in our analysis, the migration space configuration did change with each sea level rise scenario. Accordingly, the shared edge was only calculated for the first SLR scenario in which a complex was immediately adjacent with its migration space and served as the baseline connection for the other SLR scenarios.

Figure 4.3. Shared upland edge between a tidal marsh complex and its migration space. At site A, most (76%) of the marsh complex's upland edge is shared with migration space at a SLR of 0.5 feet. In contrast, site B does not have much future marsh area at the 0.5-foot scenario with only 17% of its upland edge adjacent to migration space.

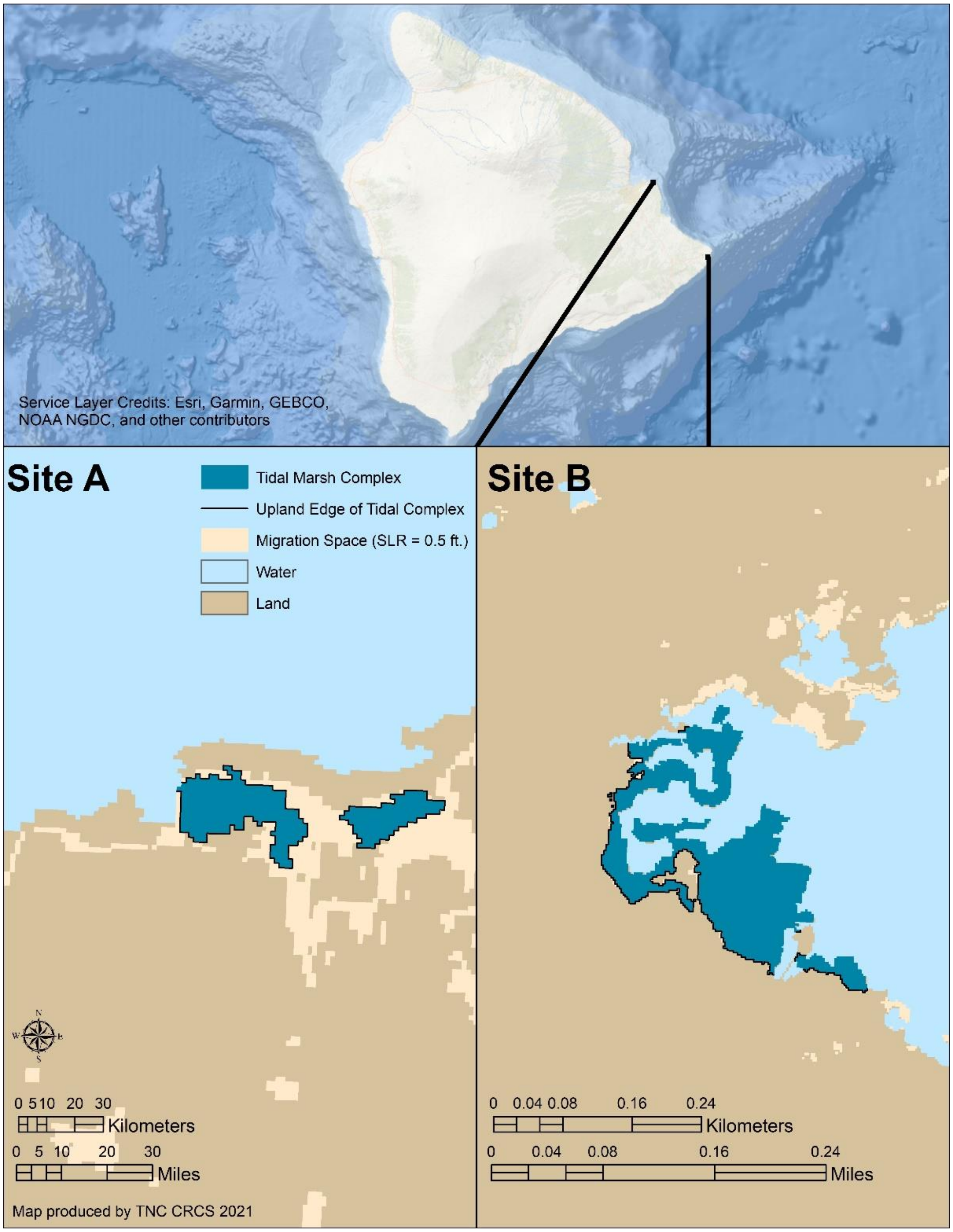

Physical Characteristics of the Existing Tidal Complex

SIZE OF EXISTING TIDAL COMPLEX (WEIGHT = 2): The size of the existing tidal complex (Figure 4.4) is likely to influence its ability to migrate because large complexes provide large sources of biotic material such as propagules and rhizomes. We gave this metric a low weight for influence, however, because most tidal complexes are already decreasing in size due to inundation and are not stable over the next century (Ganju et al., 2017). Researchers have found that aboveground and belowground biomass of *Spartina sp*. decreases exponentially with increased flood duration and higher salinities, and that even subtle increases in sea level may lead to substantial reductions in productivity and organic accretion (Snedden et al., 2015).

Figure 4.4. Tidal marsh size. The map shows different tidal marsh complexes near Kaunakakai in central Moloka'i, ranging in size from very small (< 1 acre) to large (>1000 acres).

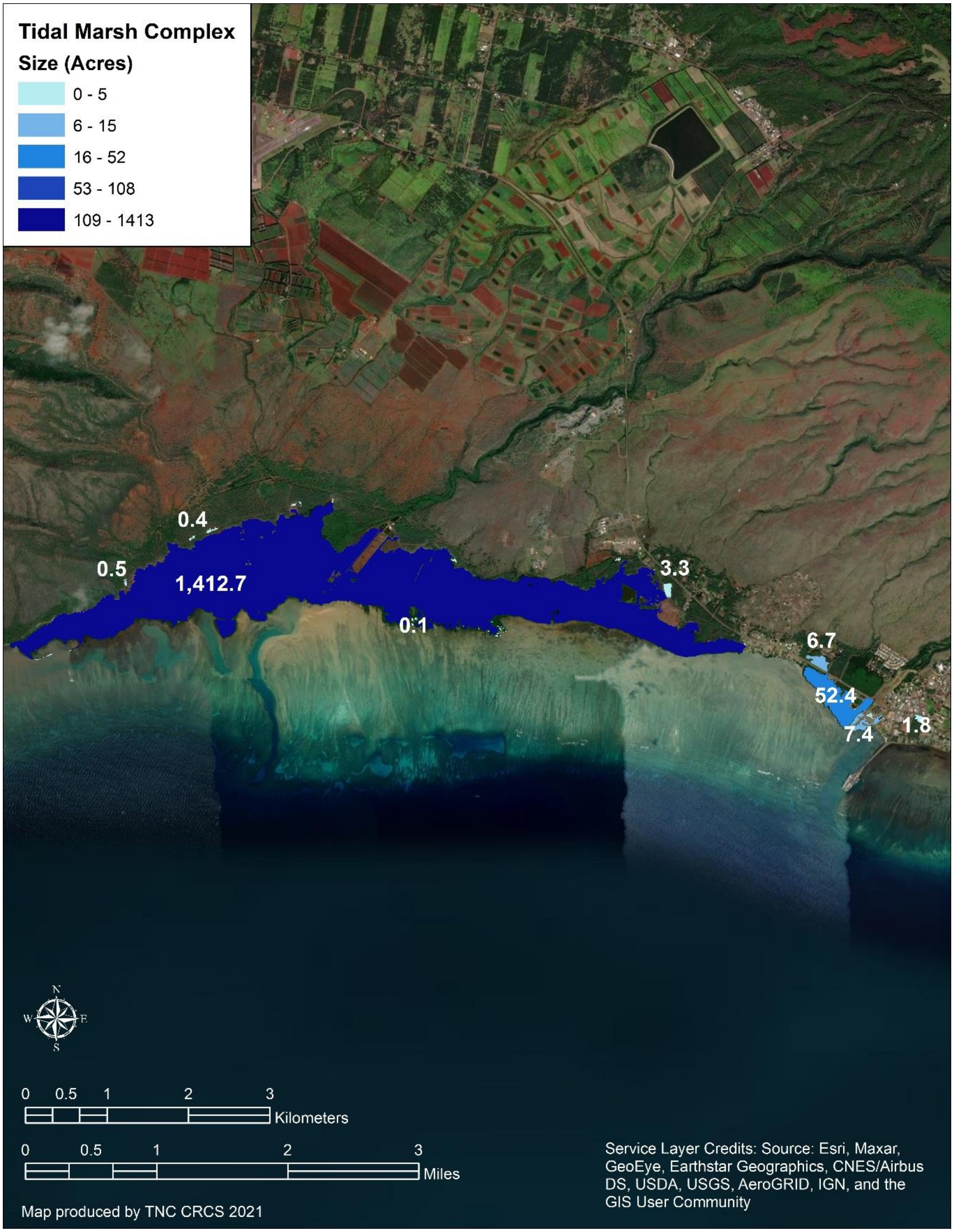

Condition Characteristics

Condition factors are characteristics that increase the probability of a tidal complex moving into its migration space and establishing new habitat. While the physical factors focus on the size and configuration of the migration space, condition factors focus on the processes that enable the migration or formation of new tidal habitats. Migration of a tidal complex can be obstructed by many things: development, barriers, degraded substrate, an inadequate sediment supply, or poor water quality that hampers normal vegetation growth. The condition metrics are designed to help determine if the migration space is usable, and whether the expected ecological processes are functioning. In this analysis, we focused only on the condition of a tidal complexes upland edge to facilitate upslope migration. We were unable to assess water quality, flow alteration, and sediment inputs for tidal complexes and anchialine pools, but these characteristics could be important for managers to consider when developing management, restoration, and conservation plans to accommodate sea level rise at individual sites.

Current Condition of the Existing Tidal Complex

DEVELOPED UPLAND EDGE: Tidal complexes with a large portion of their landward edge flanked by roads, buildings, parking lots or other anthropogenic barriers will have limited to no access to their migration space and will be unable or severely restricted in their ability to migrate upland.

For each island, we first created a development polygon by extracting all developed pixels from the NOAA 2010 C-CAP land cover grids and converting those pixels to polygons. We then intersected the upland edge of each tidal complex with the development polygon to calculate the percent of a complex's total upland edge that was developed (Figure 4.5).

Figure 4.5. Tidal complex developed upland edge. We used the percent of a complex's upland edge that was developed to assess the potential of a marsh to access its migration space. At Site A on the eastern shore of Lana'i, the upland edge (black line) of the unconsolidated shore complexes have no development separating the complexes from their migration space. In contrast, the upland edge of the Site B complex is 56% developed (red line) which will likely impact the ability of the complex to move into its migration space.

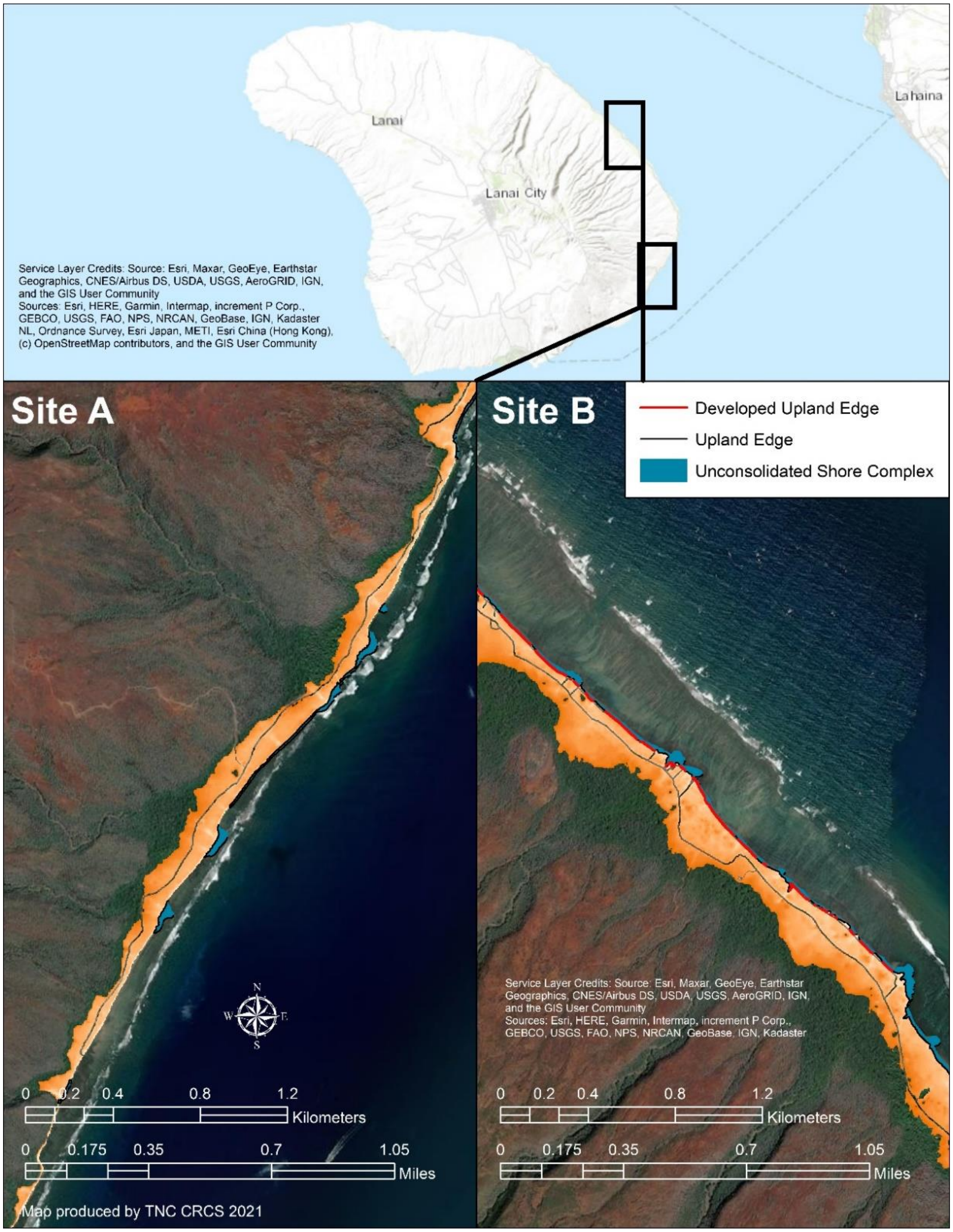

Integration of Physical and Condition Characteristics:

The final score for the tidal complex and its migration space was calculated for each site using a weighted sum of the physical and current condition characteristics along with an adjustment for migration space trend.

Weighted Sums

To put the metrics onto a standard scale, each individual variable was converted to a Z-score (standard normal distribution) relative to all sites by individual Hawaiian Island. To do this, we examined the distribution of each variable for each island. If the distribution was normal, we calculated the mean and standard deviation and used these to transform the values to standard normal (value – mean / standard deviation). If the distribution was skewed or otherwise distorted, we used various transformations to convert it to a normal distribution.

When all the variables were on the same scale, we applied the following variable weights.

Physical Options	Current Condition
Size of Migration Space (5)	Developed Upland Edge
Shared Upland Edge (2)	
Size of Complex (2)	
Weighted Sum = Physical Score	Weighted Sum = Condition Score

A score was calculated for each theme using the following equations:

*Physical Score = (5*MS + 2*SE + 2*CS)/9*

Where MS = size of migration space Z-score, SE = shared upland edge Z-score, and CS = size of complex Z-score

Condition Score = DE

Where DE = developed upland edge Z-score

Site Score
If a tidal complex's developed upland edge Z-score was less than or equal to zero (low "Average" for each Island), the physical and condition score were weighted equally and summed to calculate a site score as follows:

(Physical Score + Condition Score)/2

If a site's upland edge had little to no development (Z-score > 0), the site score was simply the Physical Score.

For anchialine pools, we used the z-score for the amount of migration space at 6.5 feet of SLR as the final resilience score.

Resilience Scores
The final scores are in standard normal units (z-scores) relative to each island. To create the final scores, we calculated the mean and variance of site resilience scores for each island (z-scores have a mean of 0 and standard deviation of 1). Use of this scheme assumed that the scores followed a normal distribution with a mean and standard deviation that accurately summarized the data. We grouped the scores into the following categories, which are used throughout the results section and serve as the legend for the various maps:

- Far Above Average (>2 standard deviations) - Most Resilient
- Above Average (1- 2 standard deviations) - More Resilient
- Slightly Above Average (0.5 to 1 standard deviations) - Somewhat Resilient
- Average (-0.5 to 0.5 standard deviations) - Average
- Slightly Below Average (-0.5 to -1 standard deviations) - Somewhat Vulnerable
- Below Average (-1 to -2 standard deviations) - More Vulnerable
- Far Below Average (<-2 standard deviations) - Most Vulnerable

Following this scheme ensured that the results were seamless across the Hawaiian Islands and allows comparisons with our terrestrial resilience analysis.

The results we present in the next chapter focus on both the 6.5-foot scenario, and the 6.5-foot scenario with trend for tidal complexes, as these provide the most comprehensive estimate of a site's resilience over the next century. However, we calculated scores for each of the twenty SLR scenarios, and these results are available to download from the project web site.

Resilience with Trend

Some sites show an increasing trend in their migration space where the amount of area gets larger within each SLR scenario. We used linear regressions to identify sites with a statistically significant ($p < 0.05$) relationship between the sea level rise scenarios (0.5 – 10 ft.) and migration space size. Sites with a significant migration space trend were assigned to one of three trend categories: increase, decrease, no change. Sites whose migration space showed an increasing trend were awarded an additional 0.50 SD points to their estimated resilience score, shown in the data as “resilience score with trend.” The remaining sites with no significant positive relationship between migration space size and SLR scenario were not penalized. The use of 0.50 SD to calculate the resilience score with trend ensured that these sites received an increase but could not change by more than one resilience class. Figure 4.6 uses a tidal marsh complex on the island of Hawai’i to illustrate how the final resilience scores were calculated.

Figure 4.6. Calculating estimated resilience. This image shows the process used to estimate the resilience score for a tidal marsh complex, outlined in black, near Lehia Beach Park, Hilo on Hawai'i Island's eastern shore. This site had no developed upland edge, so the physical score was used as the resilience score, which was then boosted by a positive and significant trend in migration space size over time.

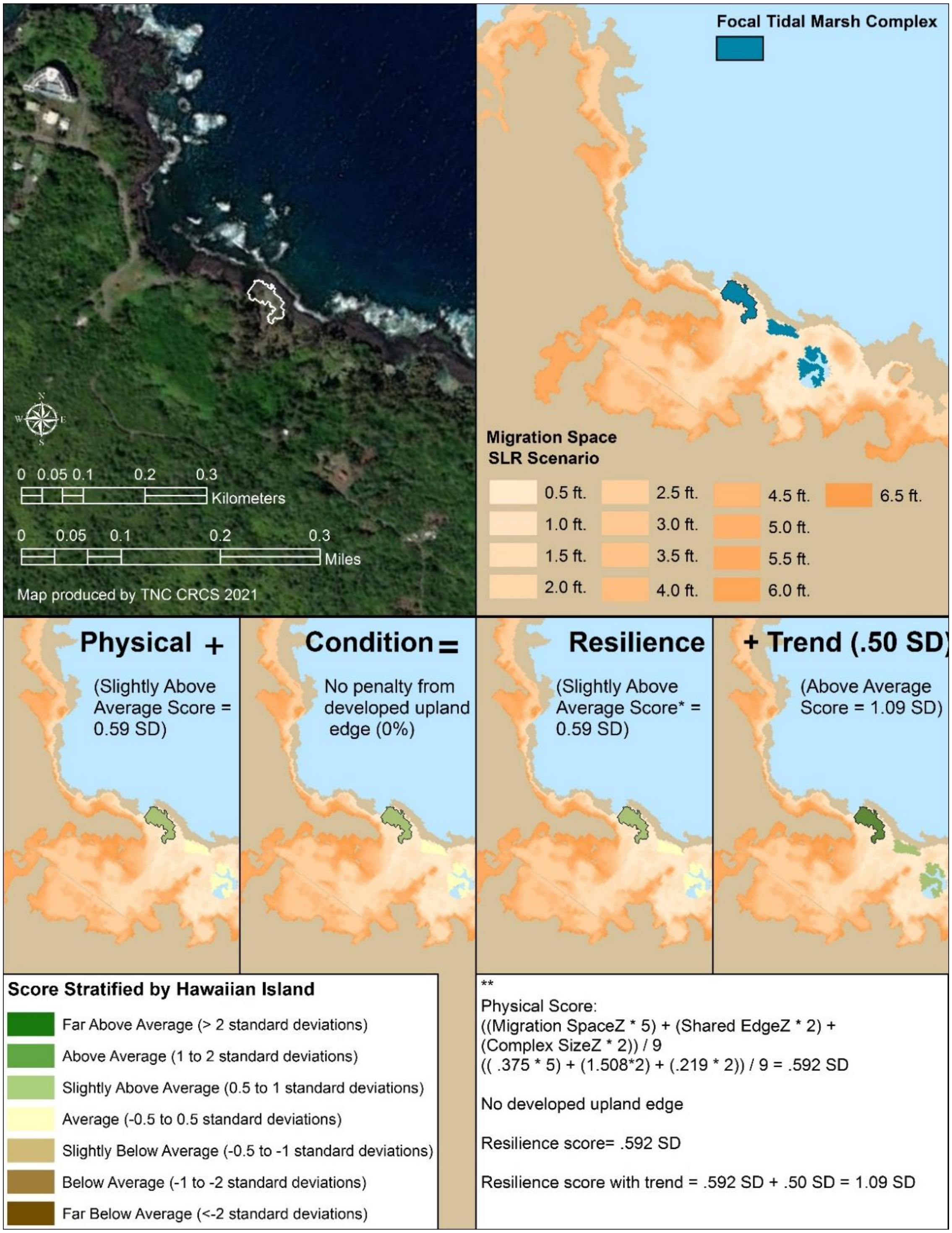

CHAPTER
5

RESULTS

This section presents the results of the 6.5-foot SLR scenario for each Hawaiian Island. For tidal complexes, we calculated the physical, condition, and final resilience scores for each site under each sea level rise scenario, and we show the 6.5-foot scenario in this section as it identifies the sites likely to be robust to the most extreme events. For anchialine pools, we calculated the amount of migration space estimated for each SLR scenario and we show the results for the 6.5-foot scenario. While site-specific results vary by island, the mean migration space of tidal marshes generally reached its peak between the 6 and 7 feet SLR scenarios and then showed declines. The change in mean migration space over the twenty SLR scenarios was more varied by island for the unconsolidated shore sites. The mean migration space of anchialine pools increased over all SLR scenarios on the island of Hawai’i, but peaked at earlier SLR scenarios for Maui and O’ahu.

The six Hawaiian Islands in our analysis have approximately 4,000 acres of estuarine wetland sites but could lose up to 87% of these existing estuarine habitats under 6.5 feet of sea level rise (NOAA, 2020a). However, our analysis identifies many resilient sites where estuarine habitats could potentially increase in size through landward migration. Some islands and tidal habitats fare better than others (Table 5.1). For example, Hawai’i could have almost three times as much tidal marsh area under a 6.5-foot SLR scenario as it currently has due to marsh migration. The amount of unconsolidated shore on Lana’i and on Maui could stay relatively similar if habitats are able to migrate. In contrast, O’ahu and Moloka’i could lose more than half of their current tidal marsh habitats to inundation, even with marsh migration.

Table 5.1. Proportion of original tidal habitat area (tidal marsh or unconsolidated shore) estimated for a SLR scenario of 6.5 feet. Tidal habitat for 6.5 feet of SLR is calculated as the sum of the remaining habitat and its potential migration space for either 1) resilient sites only or 2) all sites.

	Tidal Marsh		Unconsolidated Shore	
Island	**Migration Space of Resilient Sites**	**All Migration space**	**Migration space of Resilient Sites**	**All Migration Space**
Hawai'i	2.77	3.16	---	---
Kaua'i	0.39	0.64	0.16	0.31
Lana'i	---	---	1.10	1.98
Maui	---	---	1.10	1.31
Moloka'i	0.32	0.40	0.19	1.05
O'ahu	0.46	0.61	2.55	2.83

Six and a half feet of SLR is within the realm of possibility in the next century. Based on the latest peer-reviewed research on global mean sea level rise that considers the possibility of rapid ice melt in Greenland and Antarctica, an interagency team led by NOAA recently revised the lower and upper bounds of their global and regional sea level rise scenarios for 2100 (Sweet et al., 2017). The previous scenarios ranged from 0.65– 6.5 ft. but the six new scenarios now range from 1.0 to 8.2 ft. (0.2 - 2.0 m up to 0.3 - 2.5 m). The report also found that along all US coasts except Alaska, relative sea level is expected to be greater than the global average under several of the scenarios. Hawai'i and other Pacific Islands are likely to have disproportionately higher SLR due their long distance from ice-mass loss areas (i.e., "far-field" effects; Slangen et al., 2014) and high SLR variability within the Pacific Basin from the El Nino-Southern Oscillation (ENSO) phenomenon (Perlwitz et al., 2017). Regardless of the exact increase in Hawaiian Island ocean levels by 2100, seas will continue to rise beyond 2100 and it is critical that conservation and restoration actions be undertaken now to prepare for this future reality.

Coastal Sites

Our analysis examined the potential resilience of 172 anchialine pools, 453 tidal marsh complexes, and over one thousand unconsolidated shore complexes to twenty SLR scenarios (Table 5.2). As Table 5.2 shows, estuarine marsh complexes are less common than unconsolidated shore complexes, and despite being the third largest of the six islands, O'ahu has the most of both complex types. The majority of anchialine pools occur on Hawai'i followed by Maui. The islands of Lana'i and Maui did not have any tidal marsh complexes. There was a small amount of unconsolidated shore mapped for the island of Hawai'i and it was embedded within tidal marsh pixels, so we treated it as tidal marsh and only report on tidal marsh complexes for that island.

Table 5.2. Summary of coastal sites by Hawaiian Island

Island	Anchialine Pools	Tidal Marsh Complexes	Unconsolidated Shore Complexes
Hawai'i	82	48	N/A**
Kaua'i	---	9	252
Lana'i	---	---	27
Maui	18	---	248
Moloka'i	1 (not analyzed*)	114	171
O'ahu	7	281	336
Total	**107**	**452**	**1034**

* Located beyond the 10-ft. SLR scenario, ** Not distinguished from tidal marsh

Tidal Marsh Complexes

Tidal marshes on the Hawaiian Islands are generally quite small. We did not set a minimum tidal complex size to avoid excluding small sites with the potential to expand or merge with other nearby marshes as they migrate into larger upland areas. For all islands, the smallest size class, less than one acre, was the most common for tidal marsh complexes (Figure 5.1). O'ahu featured the largest tidal marsh encompassing approximately 1,400 acres. Moloka'i and Kaua'i had the largest average tidal marsh size (Table 5.3).

Table 5.3. Summary statistics for tidal marsh size by Hawaiian Island.

	Tidal Marsh Complex Size (Acres)				
Island	**1st Quartile**	**Median**	**Mean**	**3rd Quartile**	**Max**
Hawai'i	0.12	0.33	1.18	0.93	16.32
Kaua'i	0.27	1.60	14.83	12.37	85.85
Moloka'i	0.05	0.23	16.06	1.41	1412.67
O'ahu	0.08	0.33	3.07	1.58	153.74

Figure 5.1. Frequency of tidal marsh size class by Hawaiian Island. Small size classes are shown in white and light blue colors that transition to dark blues as the tidal marsh complex size increases.

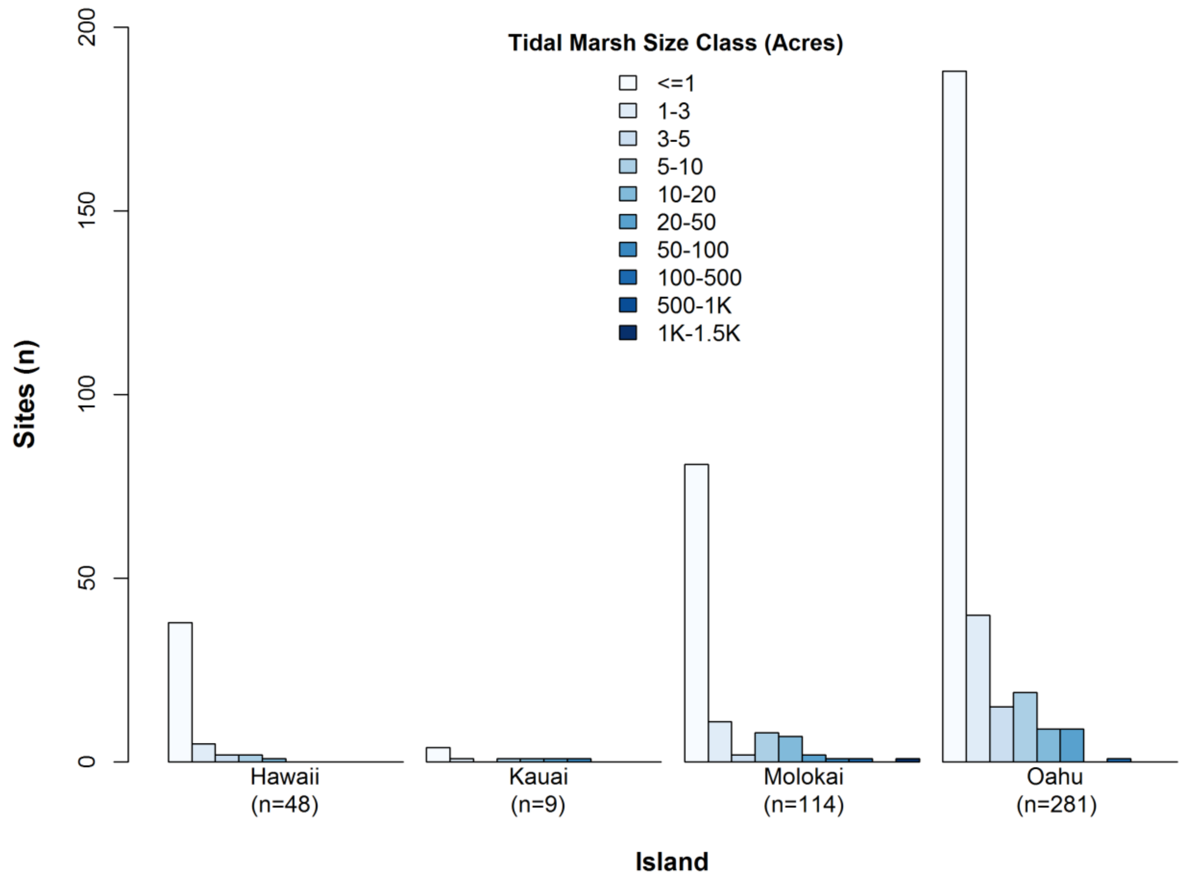

Unconsolidated Shore Complexes

Similar to tidal marsh complexes, the dominant size class of unconsolidated shore complexes was less than or equal to one acre (Figure 5.2). Lana'i had the largest average size but it was not dramatically different than the mean size of the other islands. Maui features the largest complex at 147 acres (Table 5.4). Unconsolidated shore was not differentiated from tidal marsh on the island of Hawai'i.

Table 5.4. Summary statistics for unconsolidated shore size by Hawaiian Island.

	Unconsolidated Marsh Complex Size (Acres)				
Island	**1st Quartile**	**Median**	**Mean**	**3rd Quartile**	**Max**
Kaua'i	0.08	0.37	1.26	1.00	24.68
Lana'i	0.51	1.05	4.01	3.13	27.72
Maui	0.10	0.31	1.62	0.98	146.72
Moloka'i	0.04	0.16	0.49	0.41	11.63
O'ahu	0.13	0.30	1.28	0.97	29.63

Figure 5.2. Frequency of unconsolidated shore complex size class by Hawaiian Island. Small size classes are shown in white and light blue colors that transition to dark blues as the unconsolidated shore complex size increases. Unconsolidated shore was not differentiated from tidal marsh on the island of Hawai'i, so we report on only tidal marsh complexes for that island.

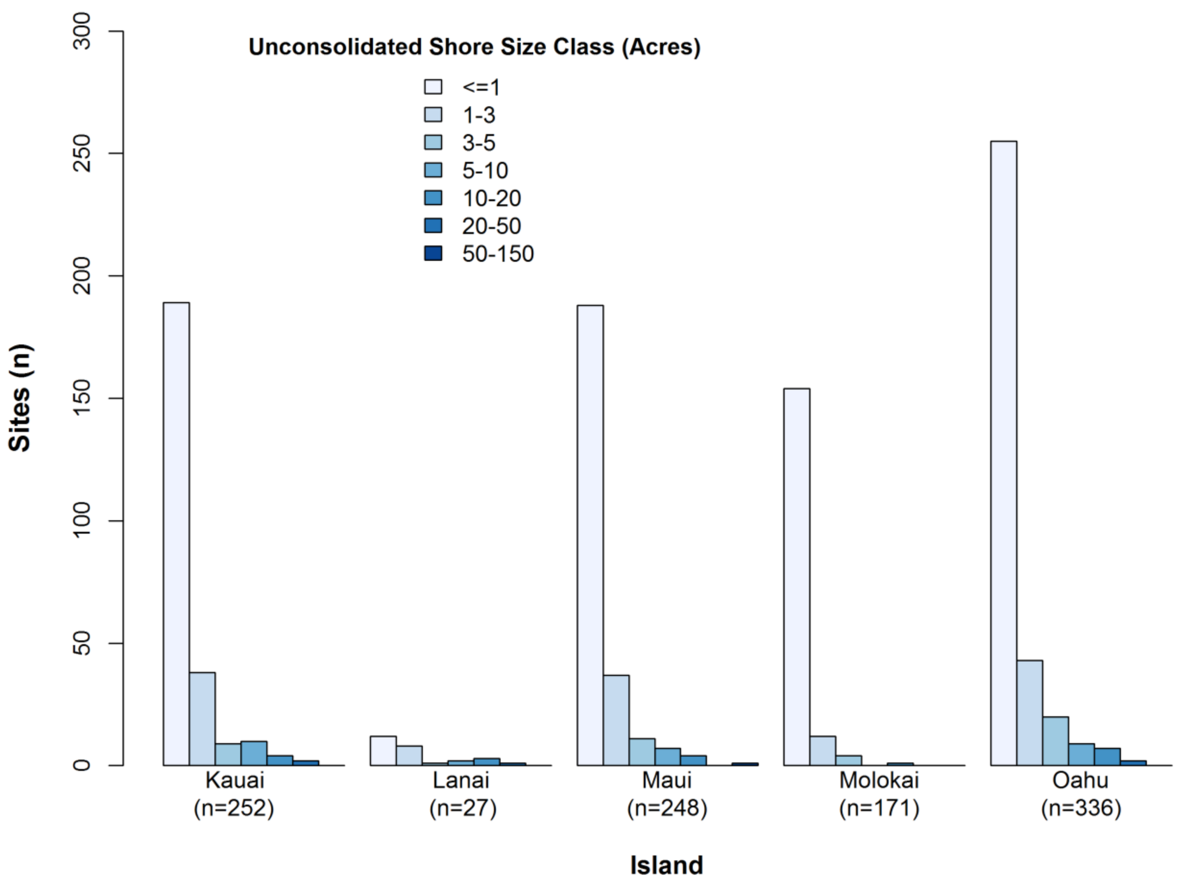

We developed 10-m landforms to identify resilient terrestrial sites for the Hawaiian Islands (Anderson et al., 2022). The landforms show the diverse topography of the islands including the low-lying coastal flat settings where the estuarine, tidal flats, and anchialine pools occur (Figure 5.3.).

Figure 5.3. Physical settings of the Hawaiian Islands.

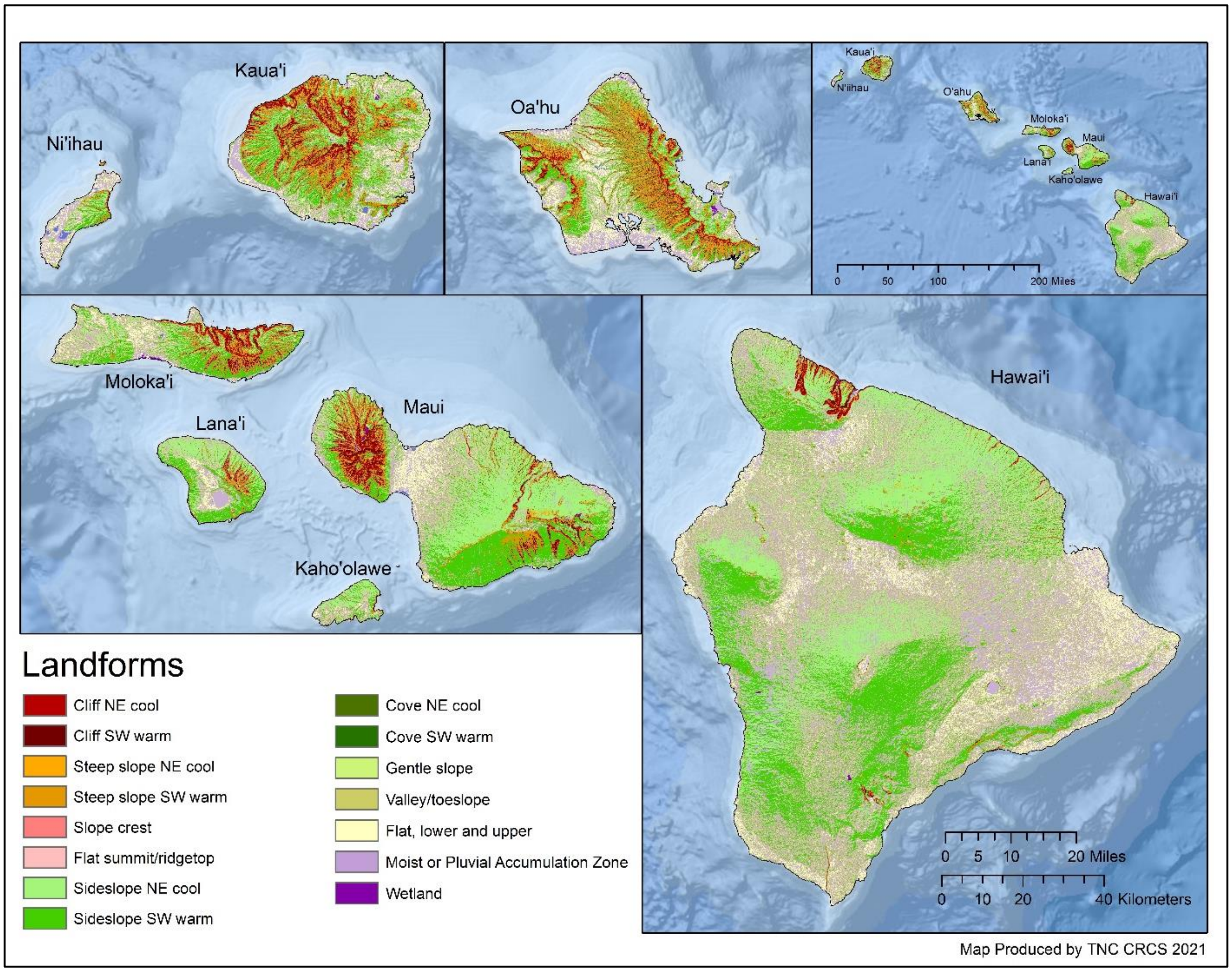

Migration Space Units

Tidal Marsh Complexes

Of the 452 tidal marsh complexes, 276 (61%), had migration space for the 6.5-foot SLR scenario. The percentage of sites with migration space was greater than 80% for both Hawai'i and Kaua'i, and was greater than 50% for Moloka'i and O'ahu (Figure 5.4). Of the four islands with tidal marsh complexes, O'ahu had the greatest number of the larger migration space size classes, followed by Moloka'i and Hawai'i (Figure 5.5). Tidal marsh sites with no migration space comprised the most frequent class on O'ahu and Moloka'i.

Figure 5.4. Percent of tidal marsh sites with migration space (SLR scenario = 6.5-ft.) by Hawaiian Island.

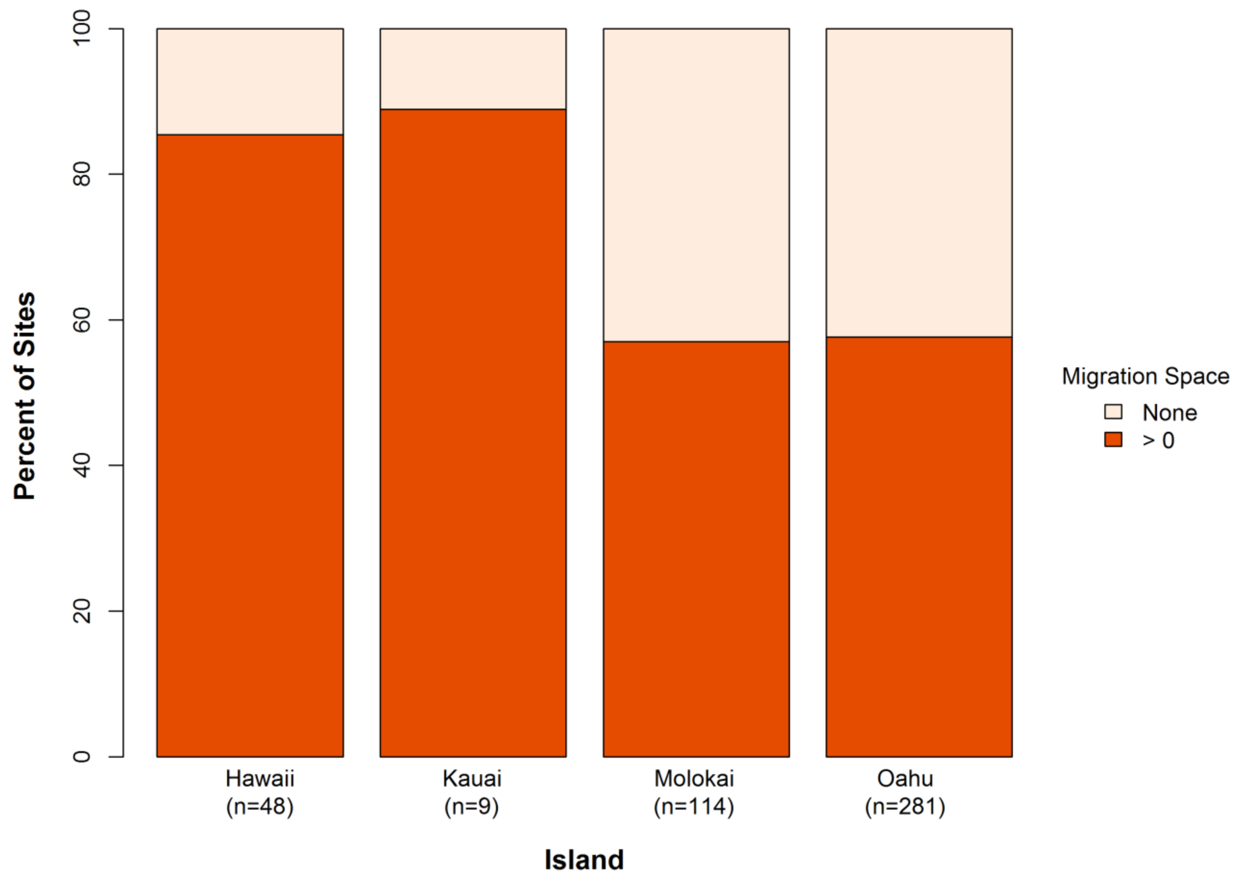

Figure 5.5. Frequency of tidal marsh migration space size class by Hawaiian Island. Small migration space size classes are shown in light yellow shades that transition to darker oranges as the migration space size increases.

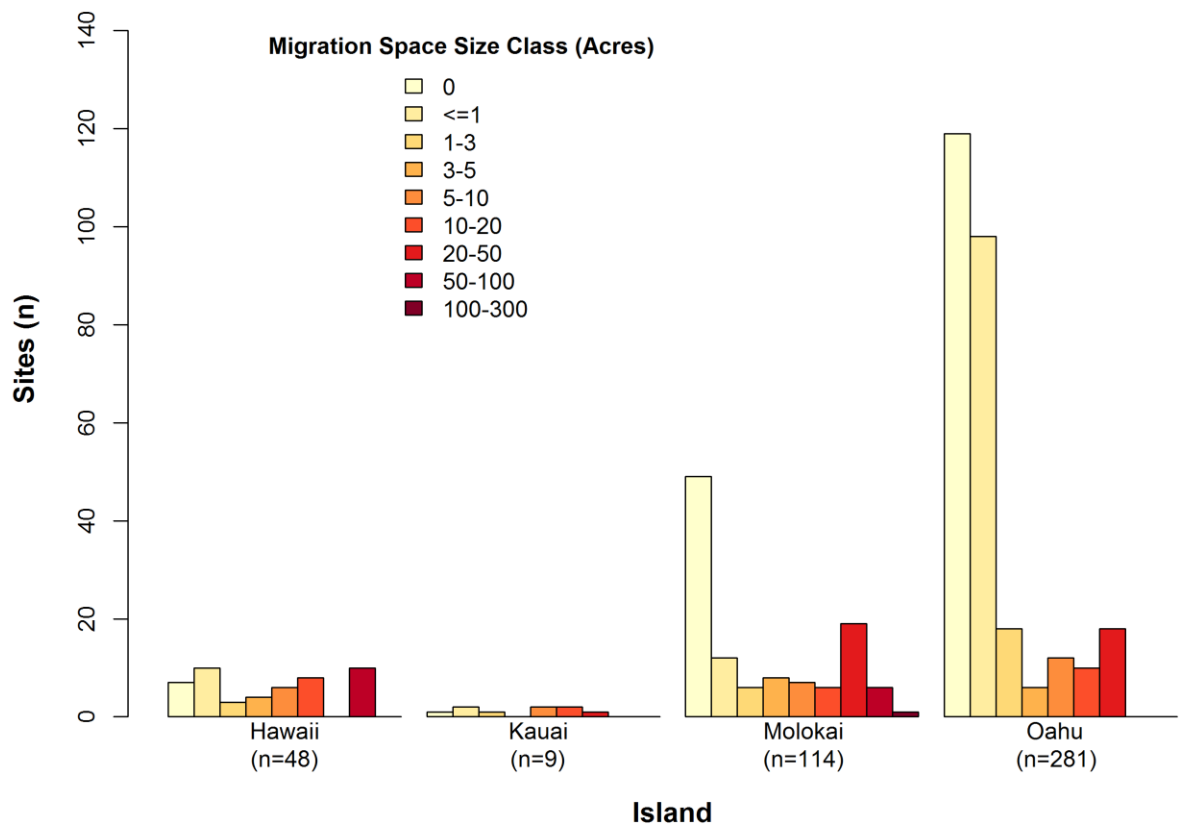

Hawai'i had the largest average migration space size while O'ahu had the smallest (Table 5.5). Moloka'i had the largest migration space at 273 acres. A Spearman's rank-order correlation showed site size and migration space size were positively correlated and this relationship was statistically significant ($r_s = 0.48$, $p < 0.0001$).

Table 5.5. Summary statistics for tidal marsh migration space size by Hawaiian Island.

	Migration Space (Acres)				
Island	**1st Quartile**	**Median**	**Mean**	**3rd Quartile**	**Max**
Hawaii	0.24	5.07	21.26	15.89	83.73
Kaua'i	0.99	6.65	9.88	16.12	35.92
Moloka'i	0.00	0.93	14.22	14.77	273.02
O'ahu	0.00	0.05	2.74	0.77	47.68

Unconsolidated Shore Complexes
Of the 1034 unconsolidated shore complexes, 924 (89%), had migration space (Figure 5.6). Of the five islands with unconsolidated shore complexes, O'ahu had the greatest number of the largest migration space size classes, followed by Moloka'i and Hawaii (Figure 5.7). Sites with less than two acres of migration space comprised the most frequent class on all islands except for Lana'i.

Figure 5.6. Percent of unconsolidated shore sites with migration space (SLR scenario = 6.5-ft.) by Hawaiian Island.

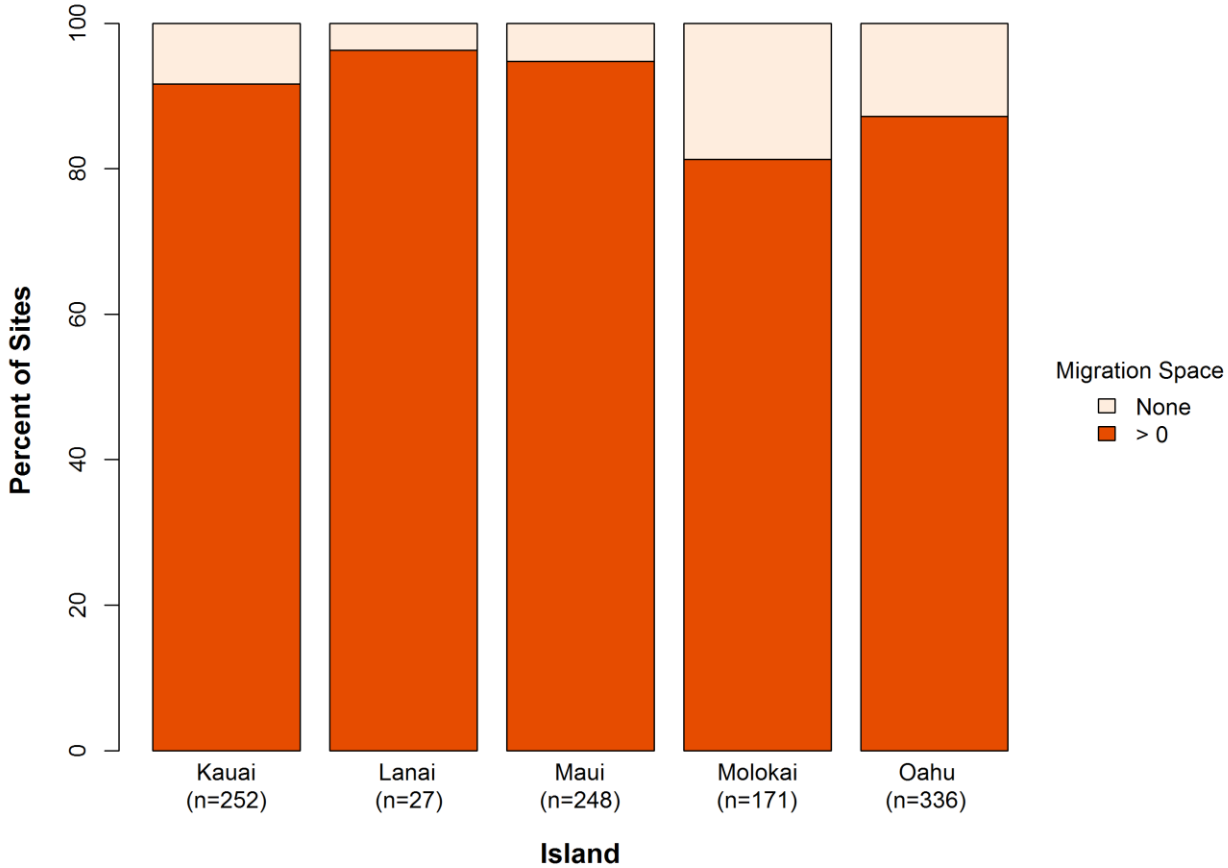

Figure 5.7. Frequency of unconsolidated shore migration space size class by Hawaiian Island. Small migration space size classes are shown in light yellow shades that transition to darker oranges as the migration space size increases. Note: unconsolidated shore was not differentiated from tidal marsh on the island of Hawai'i.

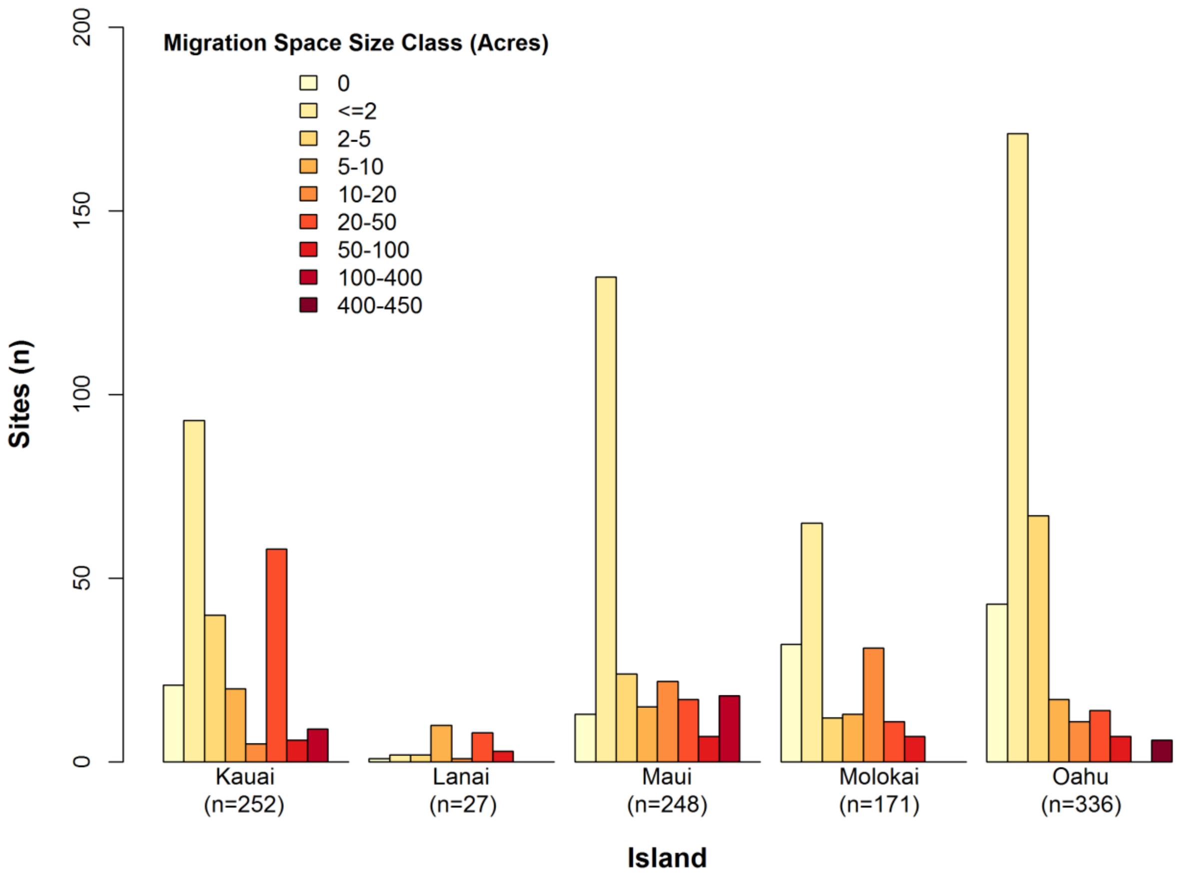

Lana'i had the largest average migration space size followed closely by Maui. Moloka'i had the smallest mean migration space size but it was not substantially smaller than the average size on Lana'i (Table 5.6). O'ahu had the largest migration space at 450 acres. A Spearman's rank-order correlation showed tidal complex size and migration space size were somewhat positively correlated and this relationship was statistically significant (r_s = 0.24, $p < 0.0001$).

Table 5.6. Summary statistics for unconsolidated shore migration space size by Hawaiian Island.

	Migration Space (Acres)				
Island	**1st Quartile**	**Median**	**Mean**	**3rd Quartile**	**Max**
Kaua'i	0.53	2.25	15.27	21.76	112.55
Lana'i	5.07	8.16	22.03	40.42	70.43
Maui	0.18	1.14	19.12	11.51	182.30
Moloka'i	0.18	1.52	9.05	12.82	90.03
O'ahu	0.06	0.79	12.37	3.18	450.02

Anchialine Pools

All anchialine pools in our analysis had migration space at a SLR scenario of 6.5 feet. Of the three islands with anchialine pools, Hawai'i had the most variation in size classes and Maui had the largest size class (Figure 5.8). Sites with less than five acres of migration space comprised the most frequent class on all three islands.

Figure 5.8. Frequency of anchialine pool migration space size class by Hawaiian Island. Small migration space size classes are shown in light yellow shades that transition to darker oranges as the migration space size increases.

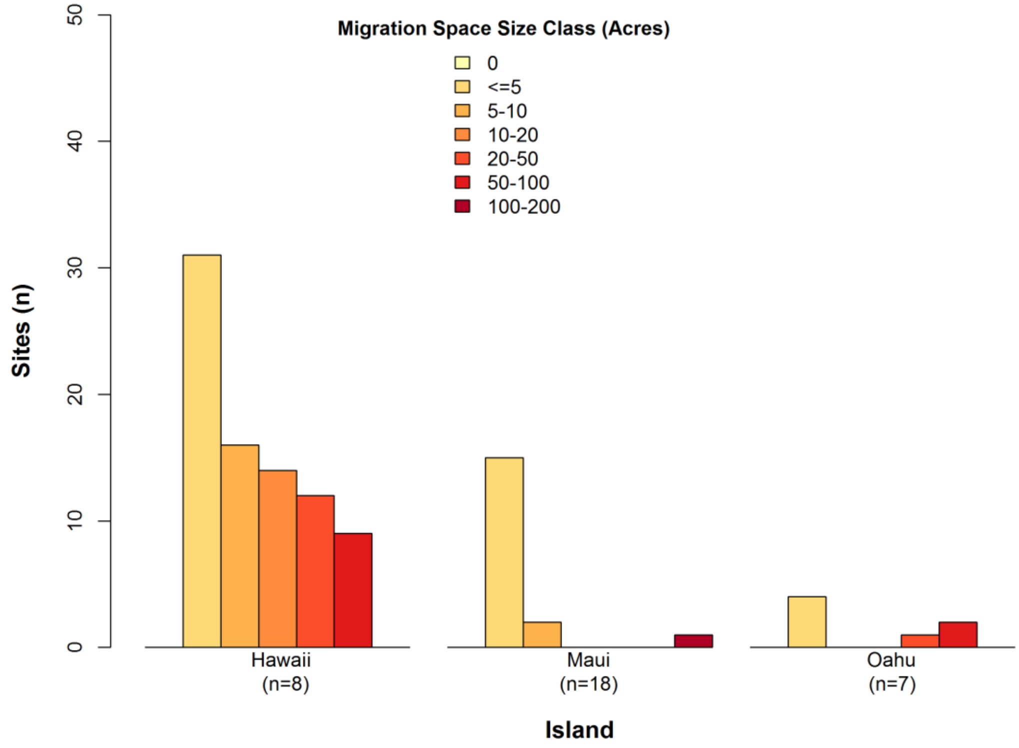

O'ahu had the largest average migration space size for anchialine pools while Maui had the largest contiguous area of migration space at 182 acres (Table 5.7).

Table 5.7. Summary statistics for anchialine pool migration space size by Hawaiian Island.

	Migration Space (Acres)					
Island	**Min**	**1st Quartile**	**Median**	**Mean**	**3rd Quartile**	**Max**
Hawaii	0.04	2.87	6.51	16.91	20.03	84.59
Maui	0.38	1.56	2.73	12.82	4.96	182.30
O'ahu	1.09	1.54	4.89	28.64	46.24	98.92

Physical and Condition Scores

For tidal complexes (tidal marsh and unconsolidated shore habitats), the estimated resilience score consists of the weighted sum of its condition and physical components (see the "Integration of Physical and Condition Characteristics" section in Chapter 4 for more details). The following section explores the developed upland edge results and the physical results for tidal marsh complexes and then unconsolidated shore complexes.

Tidal Marsh Complexes

Table 5.8 summarizes the percent of tidal marsh upland edge that is developed by Hawaiian Island. O'ahu and Kaua'i had the highest average percent development while Moloka'i had the lowest. As Table 5.8 shows, sites whose upland edge was around 10% or more developed fell in the "Average" or lower condition score classes and their condition score was used in the calculation of the resilience scores. The resilience scores of sites with less than approximately 10% (8% for Moloka'i) of their upland edge in development were based only on their physical score.

Table 5.8. Summary statistics for developed upland edge (%) of tidal marsh by Hawaiian Island. The last column shows the percent development threshold by island that corresponded to a Z-score ≤ 0. For sites that met this threshold, the condition score was combined with the physical score to calculate the resilience score.

	Tidal Marsh Developed Upland Edge (%)					
Island	**1st Quartile**	**Median**	**Mean**	**3rd Quartile**	**Max**	**Developed Upland Edge % Z-Score ≤ 0 Threshold**
Hawaii	0.00	0.00	12.53	19.06	88.64	>11%
Kaua'i	8.70	15.91	30.31	40.96	90.00	>14%
Moloka'i	0.00	0.00	9.15	12.96	100.00	>8%
O'ahu	0.00	13.33	28. 72	50.22	100.00	>13%

Table 5.9 shows the number of tidal marshes that fell into each condition class based on the amount of their upland edge that was developed. The class assignments are based on the distribution of the percent upland edge development by each Hawaiian Island.

Table 5.9. Frequency of tidal marsh condition scores for the 6.5-foot SLR scenario. The percentage of tidal marsh complexes in each condition class by Hawaiian Island is shown in parentheses. The resilience scores for marsh complexes in the dark gray classes included the physical and condition scores, while those in the unshaded classes were based solely on their physical score. The "Average" class is shaded in light gray as some of sites in this category met the ≤ 0 Z-score threshold for including condition scores.

Condition Score	Hawaii	Kaua'i	Moloka'i	O'ahu
Far Above Average	0	1 (11%)	0	0
Above Average	0	0	0	0
Slightly Above Average	33 (69%)	1 (11%)	80 (70%)	130 (46%)
Average	4 (8%)	4 (44%)	10 (9%)	54 (19%)
Slightly Below Average	4 (8%)	1 (11%)	9 (8%)	31 (11%)
Below Average	3 (6%)	2 (22%)	9 (8%)	66 (23%)
Far Below Average	4 (8%)	0	6 (5%)	0

Table 5.10 shows the number of tidal marsh sites in each physical score class. The physical score was based on a site's migration space, shared upland edge with migration space, and the existing tidal marsh size. Only Moloka'i and O'ahu had sites in the "Above Average" class and no islands had "Far Above Average" sites.

Table 5.10. Frequency of tidal marsh physical scores for the 6.5-foot SLR scenario. The percentage of tidal marsh complexes in each physical class by Hawaiian Island is shown in parentheses.

Physical Score	Hawaii	Kaua'i	Moloka'i	O'ahu
Far Above Average	0	0	0	0
Above Average	0	0	3 (3%)	16 (6%)
Slightly Above Average	10 (21%)	3 (33%)	13 (11%)	30 (11%)
Average	22 (46%)	2 (22%)	40 (35%)	84 (30%)
Slightly Below Average	6 (13%)	2 (22%)	8 (7%)	22 (8%)
Below Average	4 (8%)	2 (22%)	9 (8%)	38 (14%)
Far Below Average	6 (13%)	0	41 (36%)	91 (32%)

Table 5.11 shows how the physical and condition classes sorted out using a two-by-two frequency table. As the table indicates, there were lots of sites with “Above Average” condition scores, but that scored poorly for their physical characteristics. These were sites with no development around their upland edge but also with little to no migration space for a SLR scenario of 6.5 feet.

Table 5.11. The number of tidal marsh complexes in each physical and condition score category. A two-by-two frequency table shows the count of sites occurring in each physical and condition class combination. Physical classes are by row and condition classes are by column. Boxes shaded in gray indicate sites with the same physical and condition score class. For example, 11 marshes scored “Above Average” for both physical and condition characteristics.

	Condition Class						
Physical Class	**Far Above Average**	**Above Average**	**Slightly Above Average**	**Average**	**Slightly Below Average**	**Below Average**	**Far Below Average**
Far Above Average	0	0	0	0	0	0	0
Above Average	0	11	7	1	0	0	0
Slightly Above Average	1	36	6	9	4	0	1
Average	0	68	37	18	23	2	0
Slightly Below Average	0	6	9	10	10	3	0
Below Average	0	16	13	5	17	2	0
Far Below Average	0	107	0	2	26	3	0

Unconsolidated Shore Complexes

Table 5.12 summarizes the percent of unconsolidated shore upland edge that is developed by Hawaiian Island. Most unconsolidated shore sites on Moloka’i had no development of their upland edge. Across the islands that had both tidal marsh and unconsolidated shore sites, the average percent development was lower than that of the tidal marsh sites (Table 5.8). As unconsolidated shore sites were not surrounded by as much development as tidal marsh sites, the threshold for falling in the “Average” or lower condition class was much lower (Table 5.12).

Table 5.12. Summary statistics for developed upland edge (%) of unconsolidated shore by Hawaiian Island. The last column shows the percent development threshold by island that corresponded to a Z-score ≤ 0. For sites that met this threshold, the condition score was combined with the physical score to calculate the resilience score.

	Tidal Marsh Complex Size (Acres)					
Island	**1st Quartile**	**Median**	**Mean**	**3rd Quartile**	**Max**	**Developed Upland Edge % Z-Score ≤ 0 Threshold**
Kaua'i	0.00	0.00	3.38	0.00	96.88	> 1%
Lana'i	0.00	0.00	8.25	0.00	58.18	> 0%
Maui	0.00	0.00	5.64	0.00	100.00	> 5%
Moloka'i	0.00	14.1	0.00	0.00	100.00	> 1%
O'ahu	0.00	0.00	13.72	15.59	100.00	> 6%

As most unconsolidated shore sites had little development along their upland edge, the threshold for falling in the "Average" class was low (0-5% development, depending on the island) so most sites fell within the "Average" class (Table 5.13).

Table 5.13. Frequency of unconsolidated shore condition scores for the 6.5-foot SLR scenario. The percentage of unconsolidated shore complexes in each condition class by Island is shown in parentheses.

Condition Score	Kaua'i	Lana'i	Maui	Moloka'i	O'ahu
Far Above Average	0	0	0	0	0
Above Average	0	0	0	0	0
Slightly Above Average	0	0	0	0	195 (58%)
Average	222 (88%)	22 (81%)	222 (90%)	140 (82%)	51 (15%)
Slightly Below Average	6 (2%)	1 (4%)	7 (3%)	2 (1%)	36 (11%)
Below Average	10 (4%)	1 (4%)	6 (2%)	5 (3%)	29 (9%)
Far Below Average	14 (6%)	3 (11%)	13 (5%)	24 (14%)	25 (7%)

Compared to the other islands with unconsolidated shore sites, Maui had the greatest percentage of sites that scored high ("Above Average" and "Far Above Average") for physical characteristics (Table 5.14).

Table 5.14. Frequency of unconsolidated shore physical scores for the 6.5-foot SLR scenario. The percentage of unconsolidated shore complexes in each physical class by Hawaiian Island is shown in parentheses.

Physical Score	Kaua'i	Lana'i	Maui	Moloka'i	O'ahu
Far Above Average	0	0	1 (0%)	0	0
Above Average	13 (5%)	1 (4%)	20 (8%)	8 (5%)	16 (5%)
Slightly Above Average	49 (19%)	3 (11%)	45 (18%)	26 (15%)	52 (15%)
Average	119 (47%)	17 (63%)	118 (48%)	74 (43%)	160 (48%)
Slightly Below Average	34 (13%)	3 (11%)	31 (13%)	25 (15%)	45 (13%)
Below Average	18 (7%)	3 (11%)	22 (9%)	7 (4%)	31 (9%)
Far Below Average	19 (8%)	0	11 (4%)	31 (18%)	32 (10%)

Unconsolidated shore sites were skewed towards “Slightly Above Average” and “Average” in both condition and physical characteristics (Table 5.15). The more resilient sites were the 11 sites that scored “Above Average” for physical attributes and “Slightly Above Average” to “Average” for condition.

Table 5.15. The number of unconsolidated shore complexes in each physical and condition score category. A two-by-two frequency table shows the count of sites occurring in each physical and condition class combination. Physical classes are by row and condition classes are by column. Boxes shaded in gray indicate sites with the same physical and condition score class. For example, 34 unconsolidated shore complexes scored “Slightly Above Average” for both physical and condition characteristics.

	Condition Class						
Physical Class	**Far Above Average**	**Above Average**	**Slightly Above Average**	**Average**	**Slightly Below Average**	**Below Average**	**Far Below Average**
Far Above Average	0	0	0	1	0	0	0
Above Average	0	0	11	46	1	0	0
Slightly Above Average	0	0	34	132	4	3	2
Average	0	0	102	315	29	20	22
Slightly Below Average	0	0	20	86	8	16	8
Below Average	0	0	14	39	9	9	10
Far Below Average	0	0	14	38	1	3	37

Estimated Resilience Score

Tidal Marsh Complexes
The estimated resilience scores of tidal marsh complexes for the islands of Hawaii, Kaua'i, Moloka'i, and O'ahu are mapped in Figure 5.9 with the distribution of resilience classes shown in Table 5.16. The sites on Hawai'i highlighted in Figure 5.9 are along the Aimakapa Fishpond and scored "Slightly Above Average" for resilience. The sites along the Fishpond did not have any developed upland edge so their condition score was not incorporated into the resilience score. These sites had approximately 84 acres of migration space for the SLR scenario of 6.5 feet which was "Above Average" compared to all other tidal marsh sites on Hawai'i. The complexes themselves, while small at less than two acres, were large compared to the other tidal marsh sites on the island ("Above Average"). The sites had varying amounts of their upland edge immediately shared with migration space but were all relatively low (<15%) compared to other sites on the island.

Table 5.16. Frequency of tidal marsh resilience scores for the 6.5-foot sea level rise scenario.

Resilience Score	Hawaii	Kaua'i	Moloka'i	O'ahu
Far Above Average	0	0	0	0
Above Average	0	0	2	11
Slightly Above Average	10	2	12	15
Average	21	3	35	91
Slightly Below Average	3	2	11	38
Below Average	9	2	12	42
Far Below Average	5	0	42	84

Figure 5.9. Estimated resilience score of tidal marsh complexes. This map shows the estimated resilience score for the 6.5-foot sea level rise scenario. The map shows sites that are above (green) or below (brown) the mean relative to each island. Sites in green scored greater than "Average" and are estimated to be more resilient based on their physical characteristics. Sites in yellow are "Average." Sites in brown scored less than "Average" and are estimated to be vulnerable to sea level rise and climate change. The sites highlighted on Hawai'i scored "Slightly Above Average" in resilience and their migration space is shown in orange.

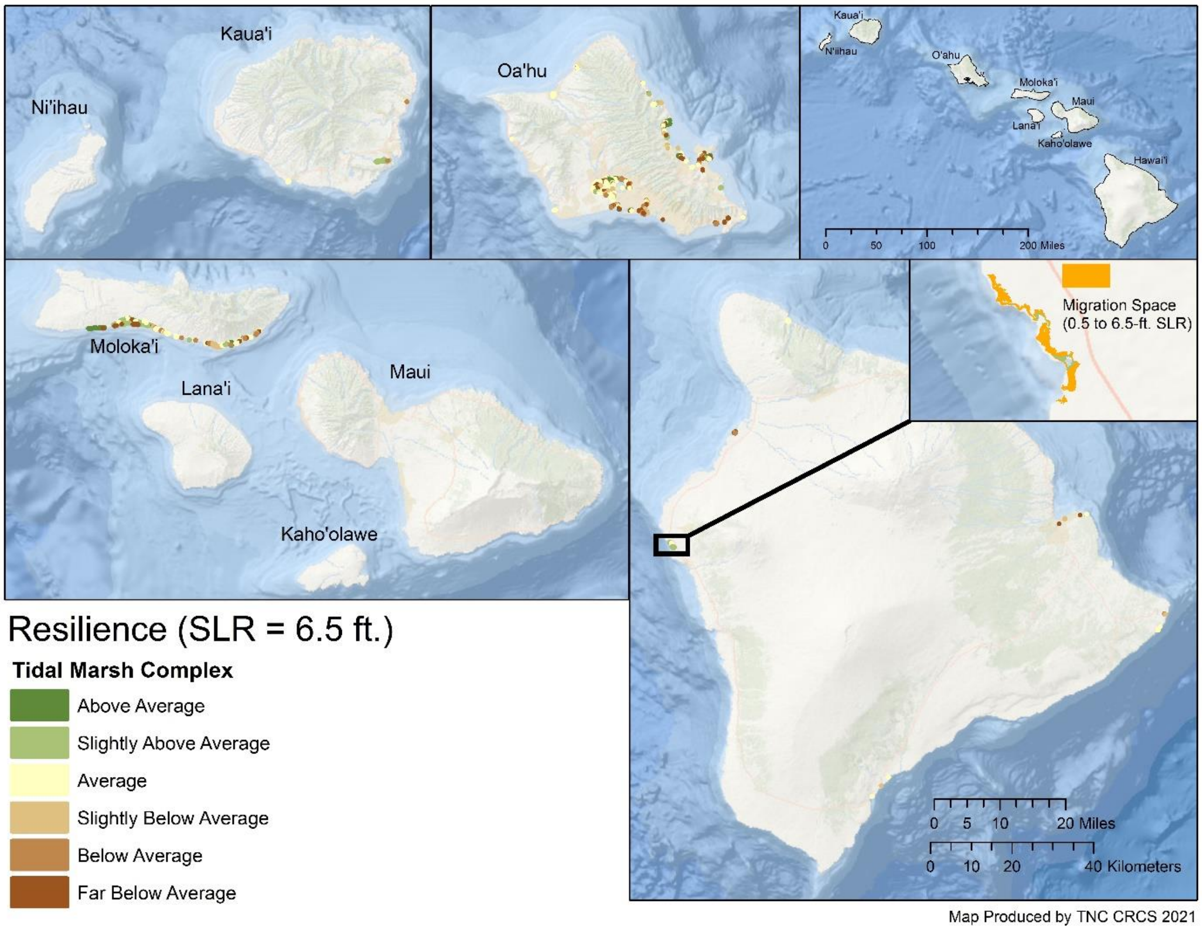

Unconsolidated Shore Complexes

The estimated resilience scores of unconsolidated shore complexes for the islands of Kaua'i, Lana'i, Maui, Moloka'i, and O'ahu are mapped in Figure 5.10 with the distribution of scores shown in Table 5.17. Across the Hawaiian Islands with tidal flat habitat, there were a number of sites that scored greater than "Average" or resilient, with Maui being the only island having a "Far Above Average" site.

The "Far Above Average" site on Maui emphasized in Figure 5.10 has 182 acres of migration space for a SLR scenario of 6.5 feet, which is "Above Average" relative to all unconsolidated shore sites on Maui. The site is located along Kealia Pond and is "Far Above Average" in size for the island at 147 acres, and the upland edge of the site has no development with 95% of it immediately adjacent to migration space ("Above Average" shared upland edge). As the site had no developed upland edge, its resilience score is based only on its physical features.

Table 5.17. Frequency of unconsolidated shore resilience scores for the 6.5-foot sea level rise scenario.

Resilience Score	Kaua'i	Lana'i	Maui	Moloka'i	O'ahu
Far Above Average	0	0	1	0	0
Above Average	12	0	19	8	14
Slightly Above Average	44	3	41	23	48
Average	110	15	117	72	147
Slightly Below Average	37	4	28	30	51
Below Average	27	5	28	6	46
Far Below Average	22	0	14	32	30

Figure 5.10. Estimated resilience score of unconsolidated shore complexes. This map shows the estimated resilience score for the 6.5-foot sea level rise scenario. The map shows unconsolidated shore sites that are above (green) or below (brown) the mean for each Hawaiian Island. Sites in green scored greater than "Average" and are estimated to be more resilient based on their physical characteristics. Sites in yellow are "Average." Sites in brown scored less than "Average" and are estimated to be vulnerable to sea level rise. The site emphasized on Maui scored "Far Above Average" in resilience and its potential migration space (182 acres) is shown in orange. Note: unconsolidated shore was not differentiated from tidal marsh on the island of Hawai'i.

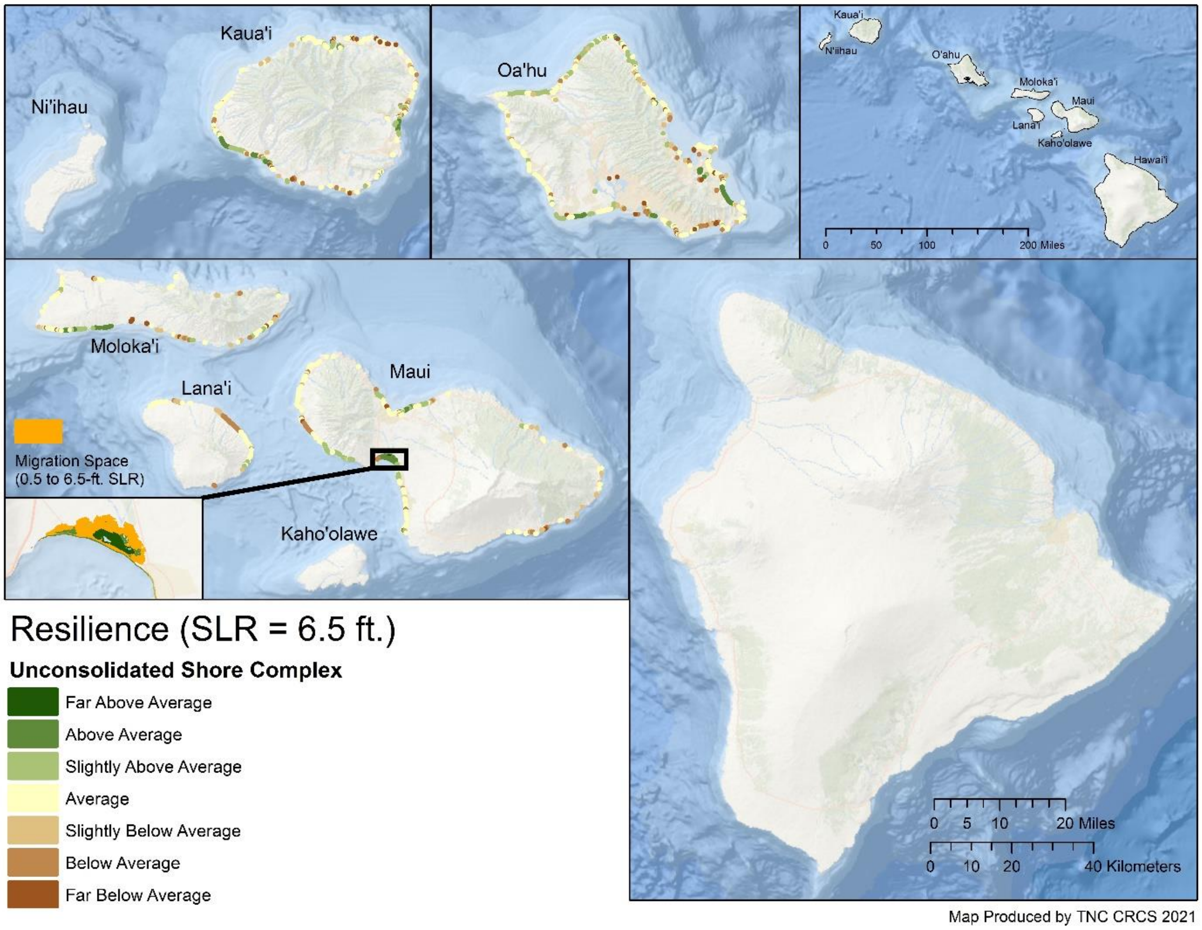

Anchialine Pools

The estimated resilience scores of anchialine pools for the islands of Hawai'i, Maui, and O'ahu are mapped in Figure 5.11 with the distribution of scores shown in Table 5.18. The resilience score of anchialine pools is based only on the estimated amount of migration space for each SLR scenario within a 100-m buffer of compatible land cover around the pool point because the extent of each pool was not available. Across the three Hawaiian Islands, there were a number of sites that scored greater than "Average" or resilient, with Maui being the only island having a "Far Above Average" site.

Table 5.18. Frequency of anchialine pool resilience scores for the 6.5-foot sea level rise scenario.

Resilience Score	Hawai'i	Maui	O'ahu
Far Above Average	0	1	0
Above Average	10	0	2
Slightly Above Average	20	6	1
Average	25	7	1
Slightly Below Average	12	1	2
Below Average	15	2	1
Far Below Average	0	1	0

Figure 5.11. Estimated resilience score of anchialine pools. This map shows the estimated resilience score for the 6.5-foot sea level rise scenario. The map shows anchialine pools that are above (green) or below (brown) the mean for the three Hawaiian Islands for which we examined anchialine pools. Sites in green scored greater than "Average" and are estimated to be more resilient based on the amount of their migration space for the 6.5-ft. SLR scenario. Sites in yellow are "Average." Sites in brown scored less than "Average" and are estimated to be vulnerable to sea level rise. The two sites highlighted on O'ahu, near the James Campbell NWR, scored "Above Average" in resilience and their potential migration space (> 60 acres) is shown in orange.

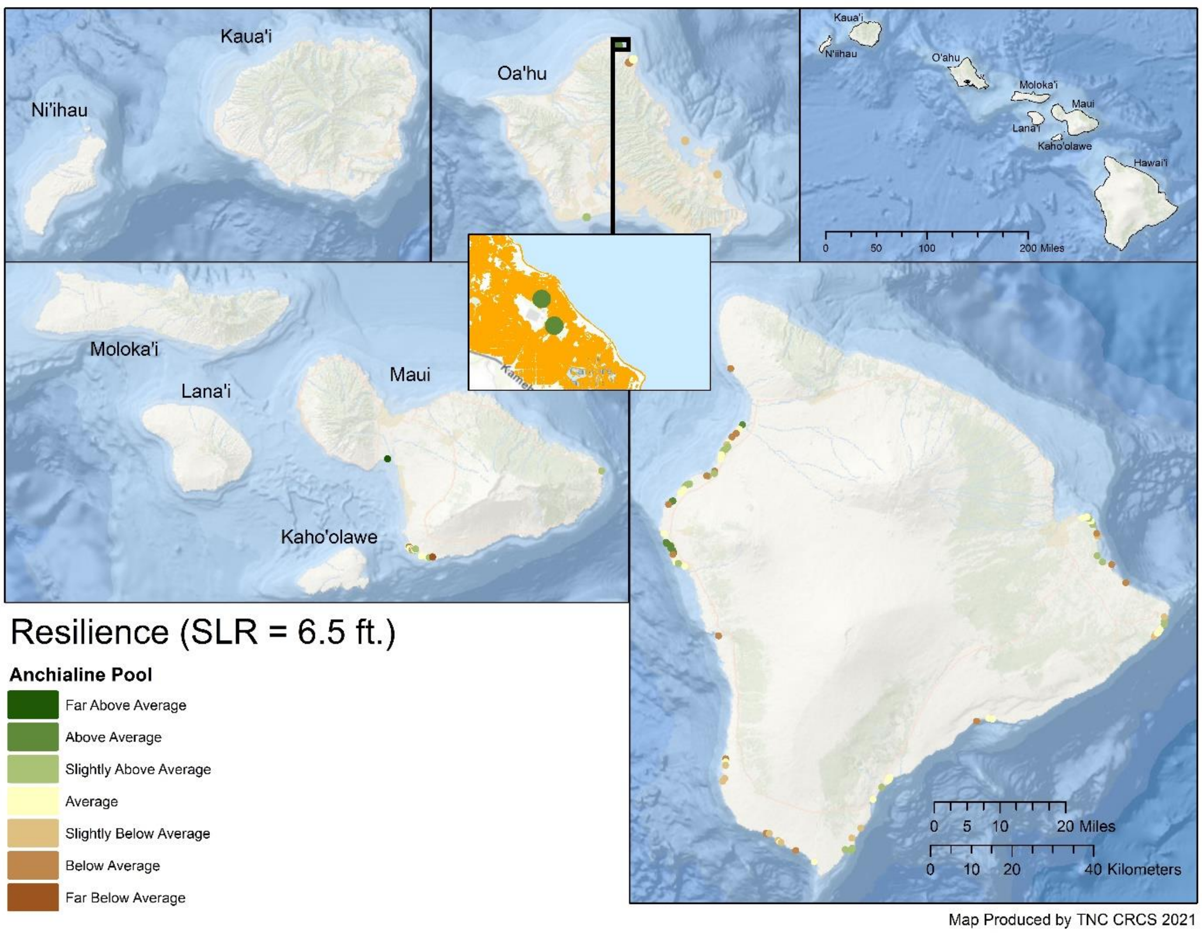

Trends in Migration Space Size

Tidal Marsh Complexes

With the exception of Hawai'i, the islands with tidal marsh complexes in our analysis experienced an increase in average migration space from the 0.5-ft. SLR scenario until the 6 to 7-foot SLR scenarios (Figure 5.12). Average migration space size peaked at the 9-foot SLR scenario for Hawai'i. Tidal marsh sites on Hawai'i also showed the largest increase in average migration space of the four islands.

Figure 5.12. Mean tidal marsh migration space size by sea level rise scenario by Hawaiian Island.

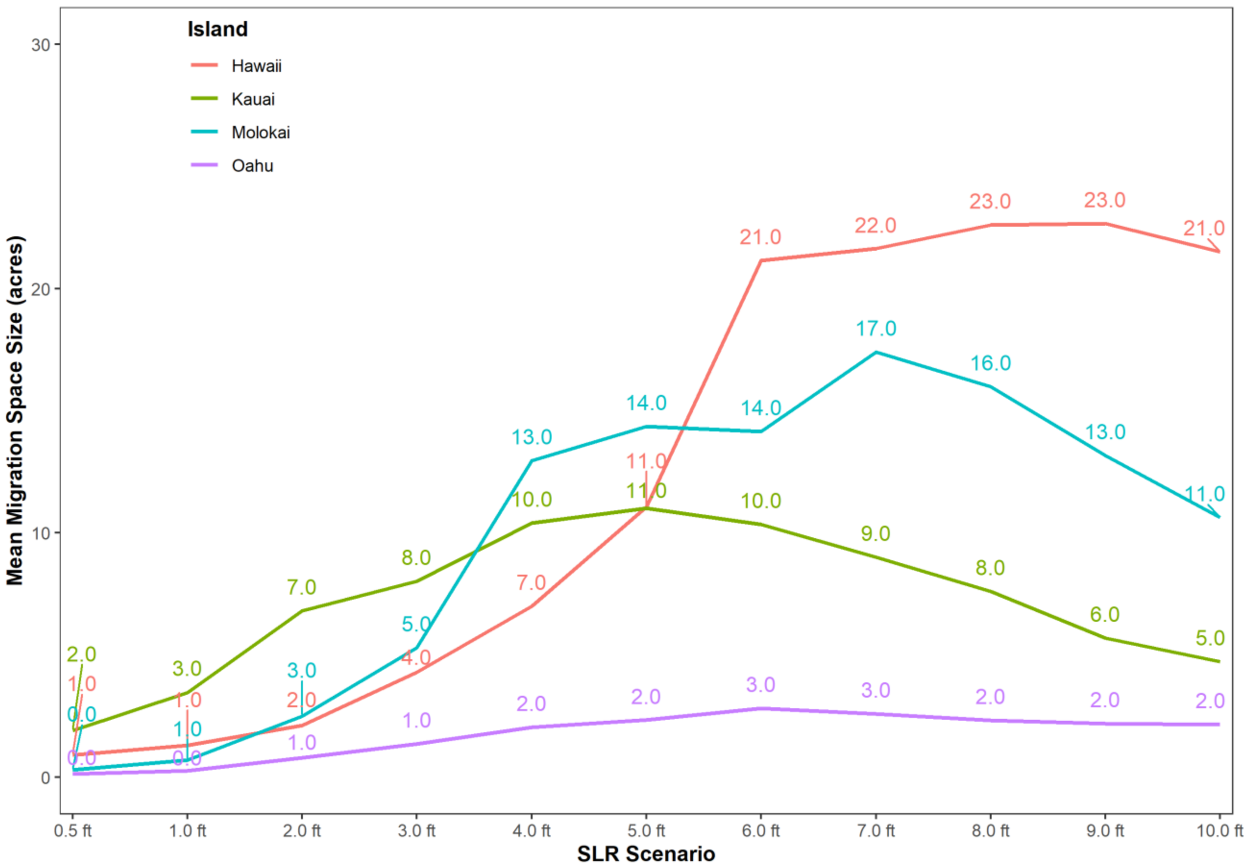

Linear regressions identified 191 tidal marsh sites with a statistically significant ($p \leq 0.05$) relationship between the sea level rise scenarios (0.5 – 10 feet) and migration space size. Of those sites with a significant relationship, 77% had increasing migration space (Figure 5.13). For the sites with a significant and increasing trend, the mean change was small across all islands (Table 5.19) with Moloka'i having the largest mean increase in size (+ .573 acres).

Table 5.19. Significant migration space trend of tidal marsh sites by Hawaiian Island. The number of tidal marsh sites with a significant ($p \leq .05$) relationship between sea level rise scenario ($\geq$ 0.5 feet) and migration space size. The mean change in migration space size (acres) for each Island is shown in parentheses next to the count of sites in each category.

Trend direction	Hawaii	Kaua'i	Moloka'i	O'ahu
Decrease	1 (-.001)	3 (-.084)	21 (-.030)	49 (-0.008)
Increase	37 (+.376)	3 (+.097)	31 (+.573)	77 (+.083)

Figure 5.13. Trend in migration space size of tidal marsh complexes by Hawaiian Island. The percent of sites on each island with an increasing or decreasing migration space trend is shown in the stacked bar plot.
0

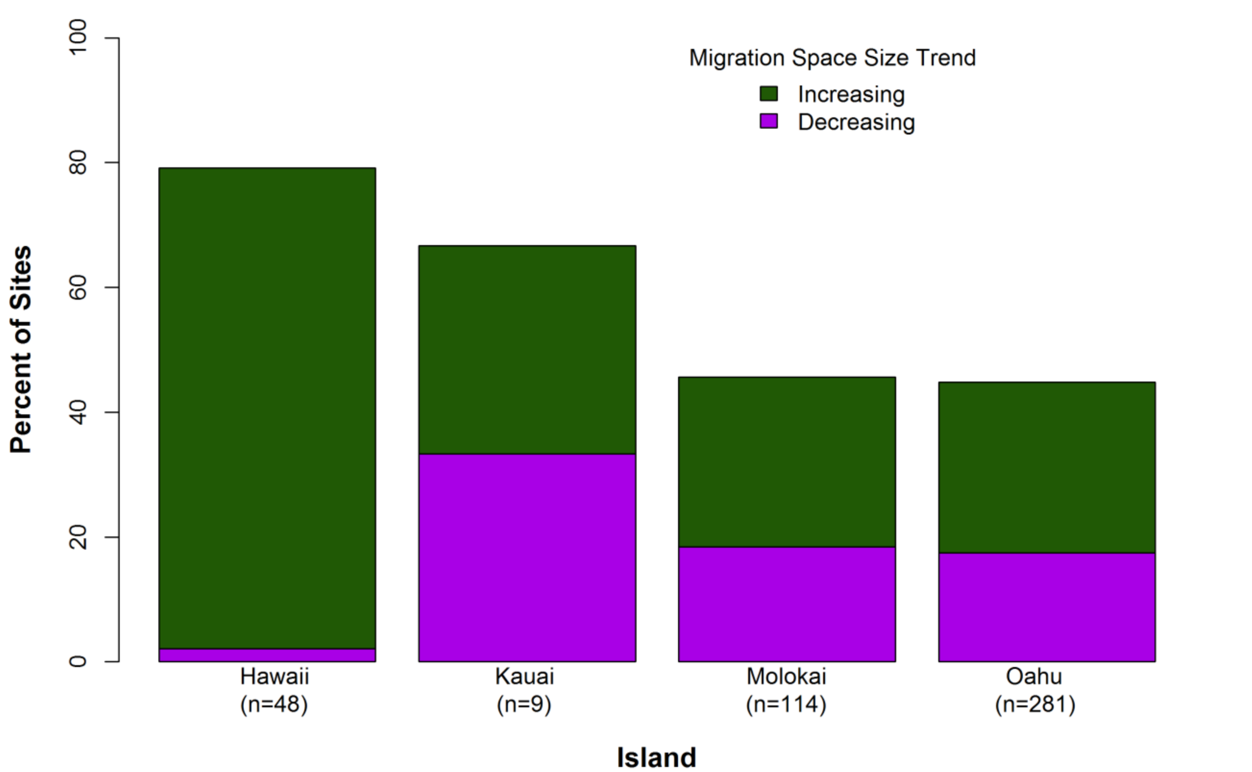

For all tidal marsh sites, 148 had migration space that showed an increasing trend, and these were awarded an additional 0.50 SD points to their estimated resilience score (shown in the dataset as “resilience score with trend”). The remaining 304 sites with no significant positive relationships between migration space size and SLR scenario were not penalized. The map in Figure 5.14 shows the spatial distribution of the tidal marsh resilience scores with the trend analysis incorporated, and Table 5.21 shows the number of sites in each resilience class by Hawaiian Island. The award was restricted such that site scores could not increase by more than one resilience class (Table 5.20). After incorporating migration space trend, 56 tidal marsh complexes moved up a class with most sites moving from “Slightly Above Average” to “Above Average” and from “Average” to “Slightly Above Average” (Table 5.20).

Table 5.20. The change in tidal class resilience class after incorporating trend in migration space size. Tidal marsh sites whose migration space showed a significant increase ($p \leq .05$) from the 0.5 to 10-foot sea level rise scenario received an additional 0.50 standard deviation units to their score. The green boxes highlight the number of sites whose class improved when the migration space trend was incorporated.

	Resilience with Trend						
Resilience Class	**Far Above Average**	**Above Average**	**Slightly Above Average**	**Average**	**Slightly Below Average**	**Below Average**	**Far Below Average**
Far Above Average	0	0	0	0	0	0	0
Above Average	0	13	0	0	0	0	0
Slightly Above Average	0	25	14	0	0	0	0
Average	0	0	29	121	0	0	0
Slightly Below Average	0	0	0	2	52	0	0
Below Average	0	0	0	0	0	65	0
Far Below Average	0	0	0	0	0	0	131

Table 5.21. Frequency of tidal marsh resilience scores for the 6.5-foot SLR scenario with migration trend.

Resilience with Trend Score	Hawaii	Kaua'i	Moloka'i	O'ahu
Far Above Average	0	0	0	0
Above Average	10	0	11	17
Slightly Above Average	12	2	14	15
Average	10	3	24	86
Slightly Below Average	2	2	11	37
Below Average	9	2	12	42
Far Below Average	5	0	42	84

Figure 5.14. Estimated resilience score with migration space trend. This map shows the estimated resilience score for the 6.5-ft. SLR scenario after incorporating the trend in migration space size. Sites whose migration space showed a significant increase ($p \leq 0.05$) from the 0.5 to 10-foot SLR received an additional 0.50 standard deviation units to their score. After incorporating the migration space trend boost, the sites highlighted on Hawai'i moved from "Slightly Above Average" in resilience to "Above Average."

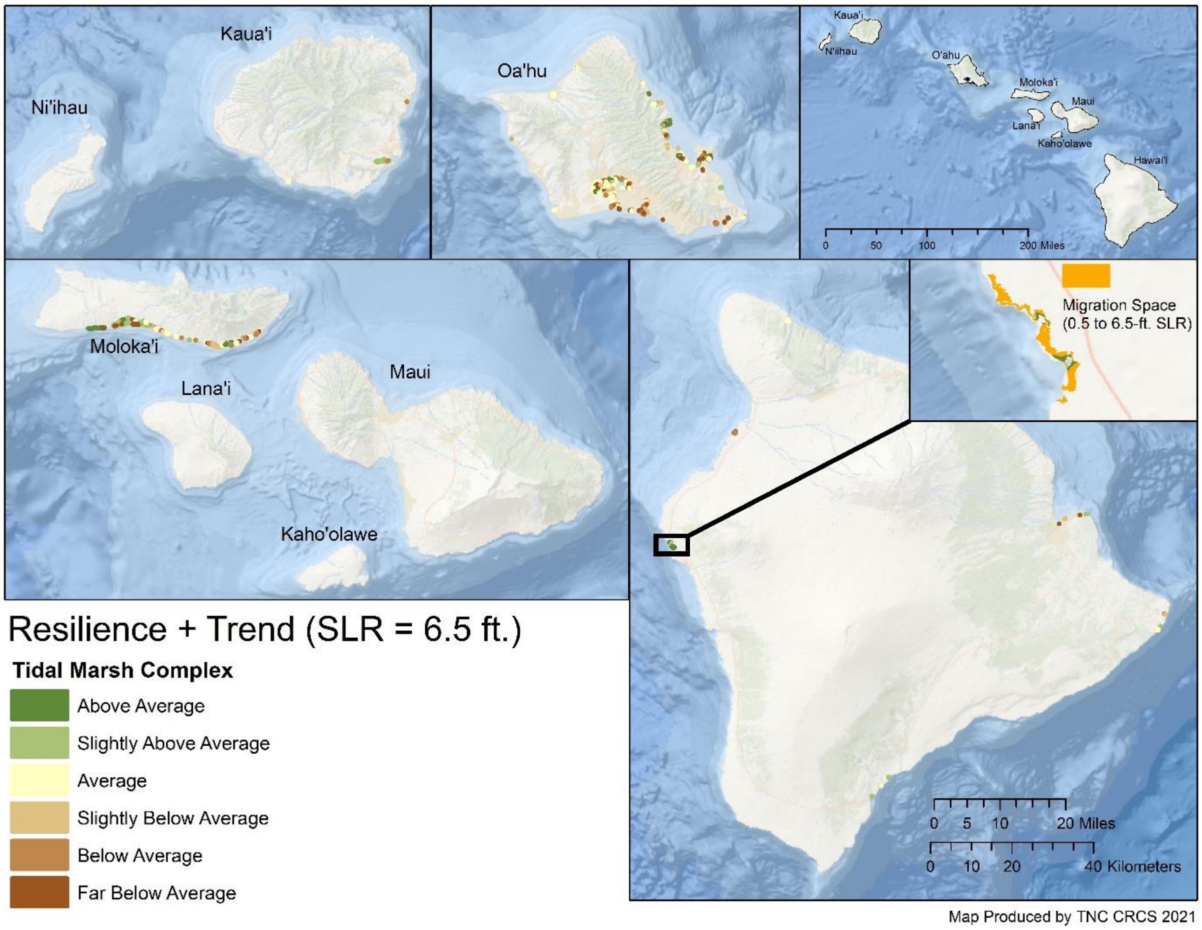

Unconsolidated Shore Complexes

The change in the average size of migration space for unconsolidated shore sites by SLR scenario varied across the five islands with peaks reached at different SLR scenarios and some islands showing increases at higher SLR scenarios (

Figure 5.15). Sites on Lana'i had the biggest increase in mean migration space up to the 8-ft. SLR scenario and then showed a substantial decline to the 10-ft. SLR scenario, while sites on Kaua'i showed a large increase from the 9 to 10-ft. SLR scenario.

Figure 5.15. Mean unconsolidated shore migration space size of unconsolidated shore sites by SLR scenario for each Hawaiian Island.

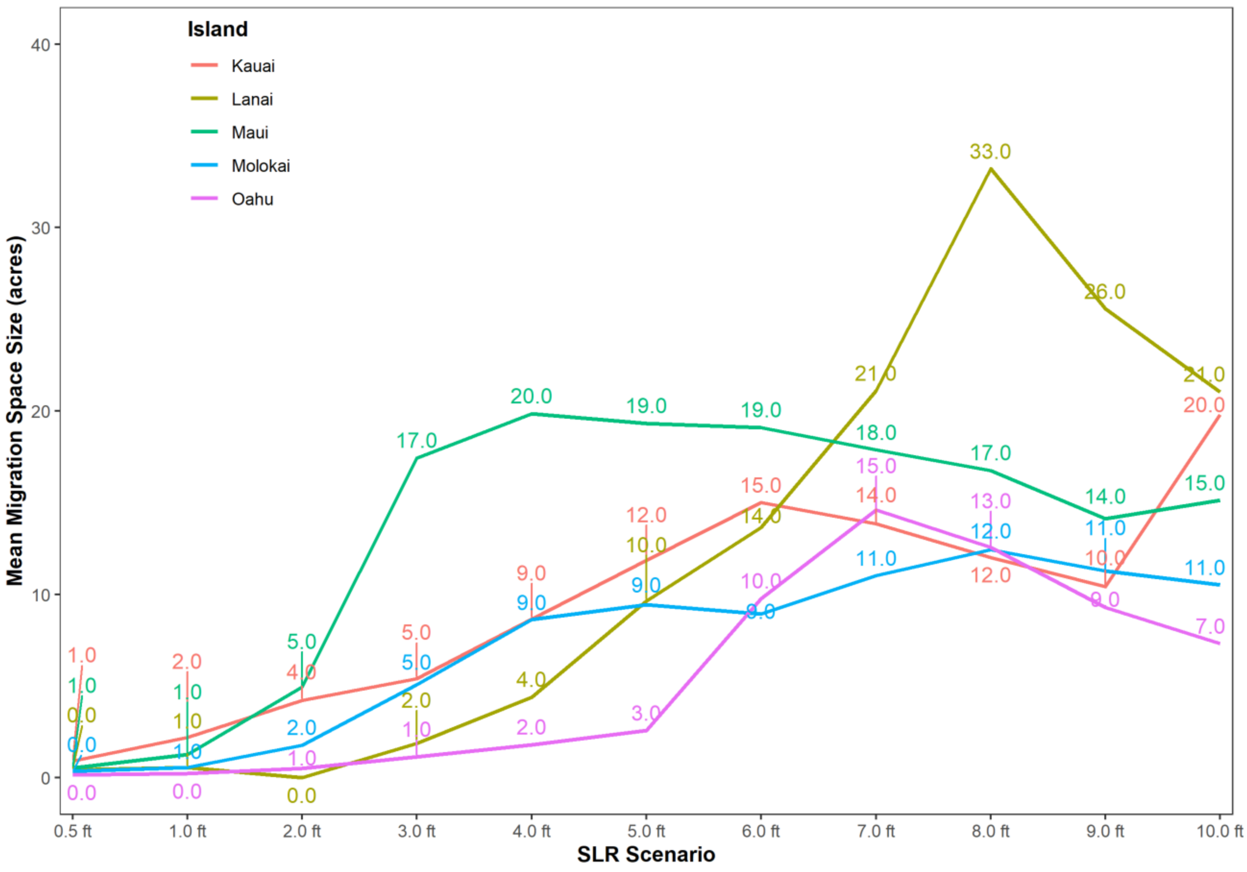

Linear regressions identified 707 unconsolidated shore sites with a statistically significant ($p \leq 0.05$) relationship between the sea level rise scenarios (0.5 – 10 feet) and migration space size. Most of the sites with a significant relationship had an increase in migration space (Figure 5.16). For those sites across all islands, the mean increase was small (Table 5.22) with Lana'i having the largest mean increase in size (+ .403 acres).

Table 5.22. Significant migration space trend by Hawaiian Island. The number of unconsolidated shore sites with a significant ($p \leq .05$) relationship between SLR scenario ($\geq$ 0.5 feet) and migration space size. The mean change in migration space size (acres) for each Hawaiian Island is shown in parentheses next to the count of sites in each category.

Trend direction	Kaua'i	Lana'i	Maui	Moloka'i	O'ahu
Decrease	27 (-.155)	1 (-.002)	10 (-.003)	13 (-.023)	27 (-.009)
Increase	166 (+.232)	24 (+.403)	149 (+.168)	93 (+.211)	197 (+.246)

Figure 5.16. Trend in migration space size of unconsolidated shore complexes by Hawaiian Island. The percent of sites on each island with an increasing or decreasing migration space trend is shown in the stacked bar plot.

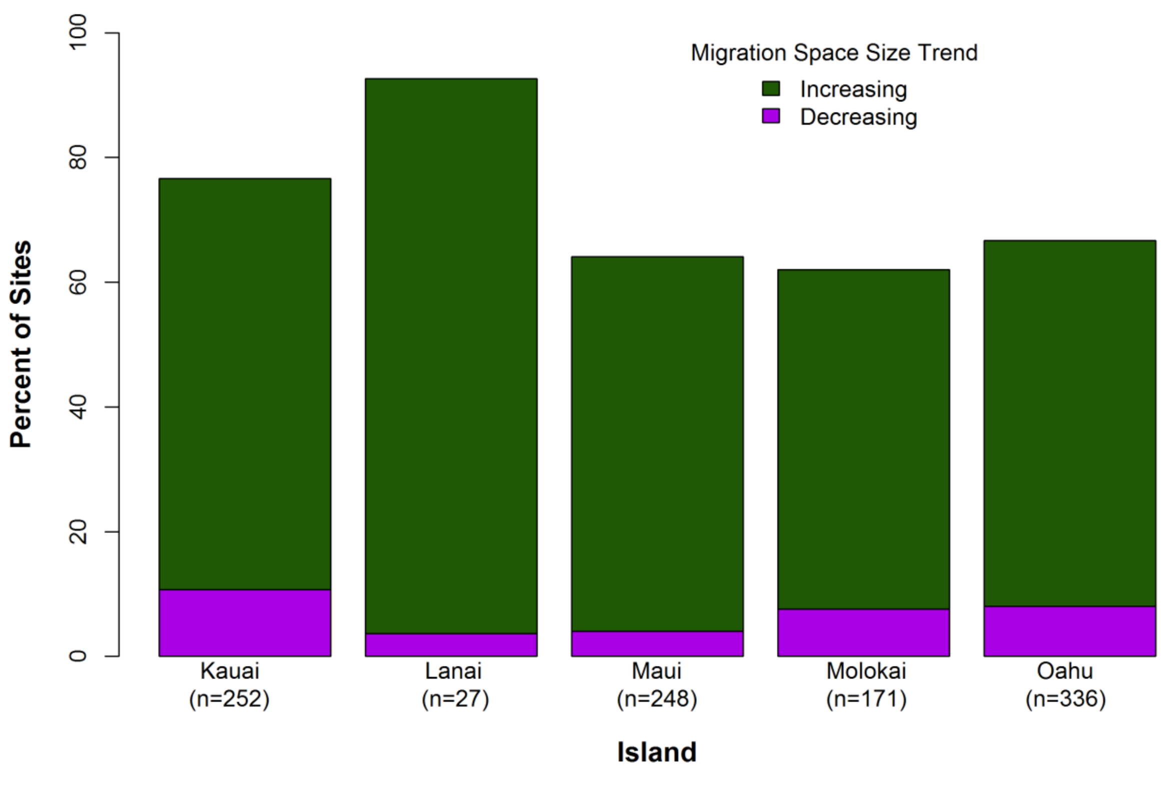

Across all islands, 629 unconsolidated shore sites had migration space that showed an increasing trend, and these were awarded an additional 0.50 SD points to their estimated resilience score (shown in the dataset as "resilience score with trend"). The remaining 405 sites with no significant positive relationships between migration space size and SLR scenario were not penalized. The map in Figure 5.17 shows the spatial distribution of the unconsolidated shore resilience scores with the trend analysis incorporated, and Table 5.24 shows the number of sites in each resilience class by Hawaiian Island. With the small bonus, site scores could not increase by more than one resilience class (Table 5.23). After incorporating migration space trend, 232 unconsolidated shore complexes moved up a class with most sites moving from "Slightly Above Average" to "Above Average" and from "Average" to "Slightly Above Average" (Table 5.23).

Table 5.23. The change in unconsolidated shore resilience class after incorporating trend in migration space size. Unconsolidated shore sites whose migration space showed a significant increase ($p \leq .05$) from the 0.5 to 10-foot SLR scenario received an additional 0.50 standard deviation units to their score. The green boxes highlight the number of sites whose class improved when the migration space trend was incorporated.

	Resilience with Trend						
Resilience Class	**Far Above Average**	**Above Average**	**Slightly Above Average**	**Average**	**Slightly Below Average**	**Below Average**	**Far Below Average**
Far Above Average	1	0	0	0	0	0	0
Above Average	4	49	0	0	0	0	0
Slightly Above Average	0	80	79	0	0	0	0
Average	0	0	106	355	0	0	0
Slightly Below Average	0	0	0	34	116	0	0
Below Average	0	0	0	0	8	104	0
Far Below Average	0	0	0	0	0	0	98

Table 5.24. Frequency of unconsolidated shore resilience scores for the 6.5-foot SLR scenario with migration trend.

Resilience with Trend Score	**Kaua'i**	**Lana'i**	**Maui**	**Moloka'i**	**O'ahu**
Far Above Average	0	0	1	0	4
Above Average	32	3	31	23	40
Slightly Above Average	50	6	46	32	51
Average	98	11	105	56	119
Slightly Below Average	31	2	23	22	46
Below Average	19	5	28	6	46
Far Below Average	22	0	14	32	30

Figure 5.17. Estimated unconsolidated shore resilience score with migration space trend. This map shows the estimated resilience score for the 6.5-ft. SLR scenario after incorporating the trend in migration space size. Sites whose migration space showed a significant increase ($p \leq 0.05$) from the 0.5 to 10-foot SLR received an additional 0.50 standard deviation units to their score. Note: unconsolidated shore was not differentiated from tidal marsh on the island of Hawai'i.

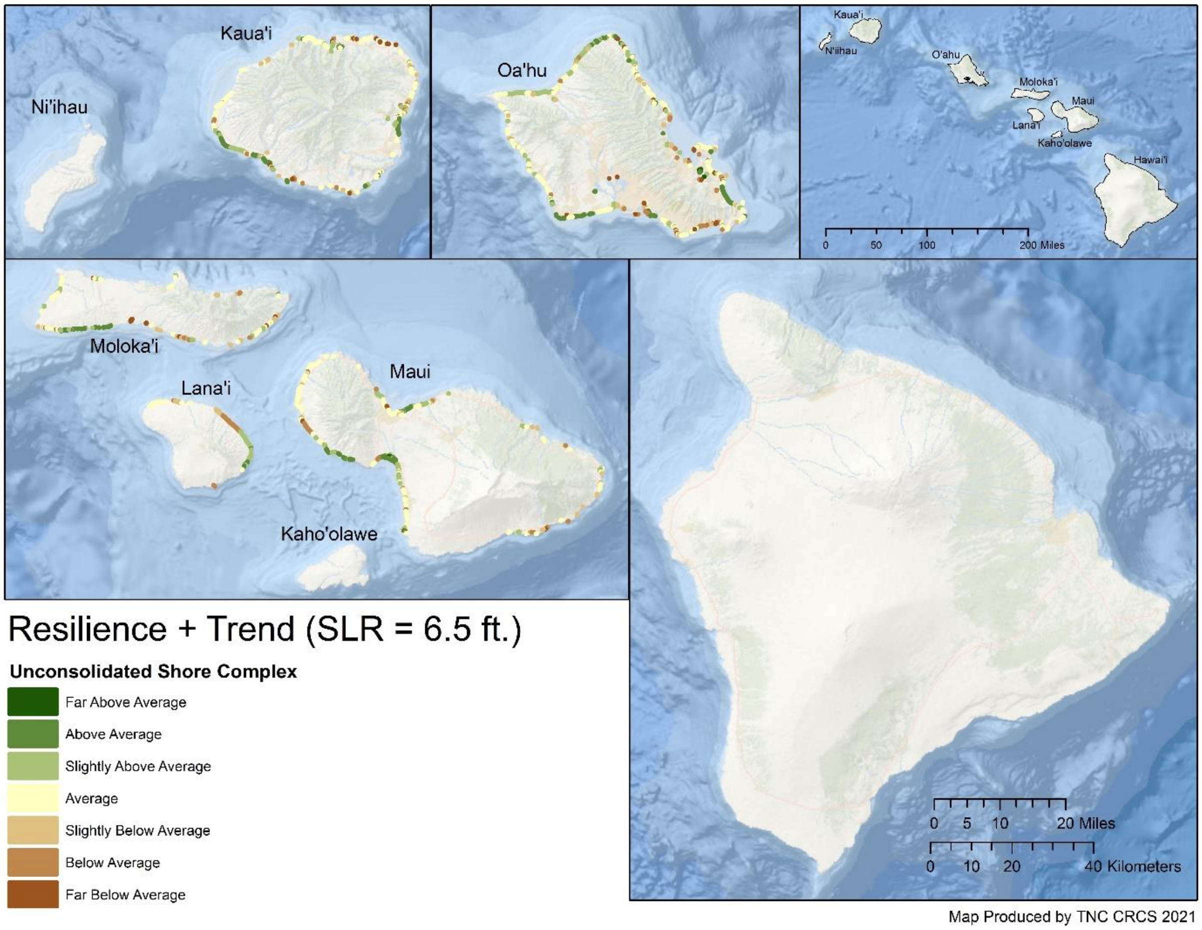

Anchialine Pools
While we did not incorporate migration space trend into the anchialine pool resilience score, Figure 5.18 shows how the mean migration space size of these pools changed over time for Hawai'i, Maui, and O'ahu. O'ahu had the greatest increase in average migration space that peaked at the 7.0-ft. SLR scenario but then declined to a lower size than that of Hawai'i, which peaked at the 10-ft. SLR scenario.

Figure 5.18. Mean anchialine pool migration space size by SLR scenario for each Hawaiian Island.

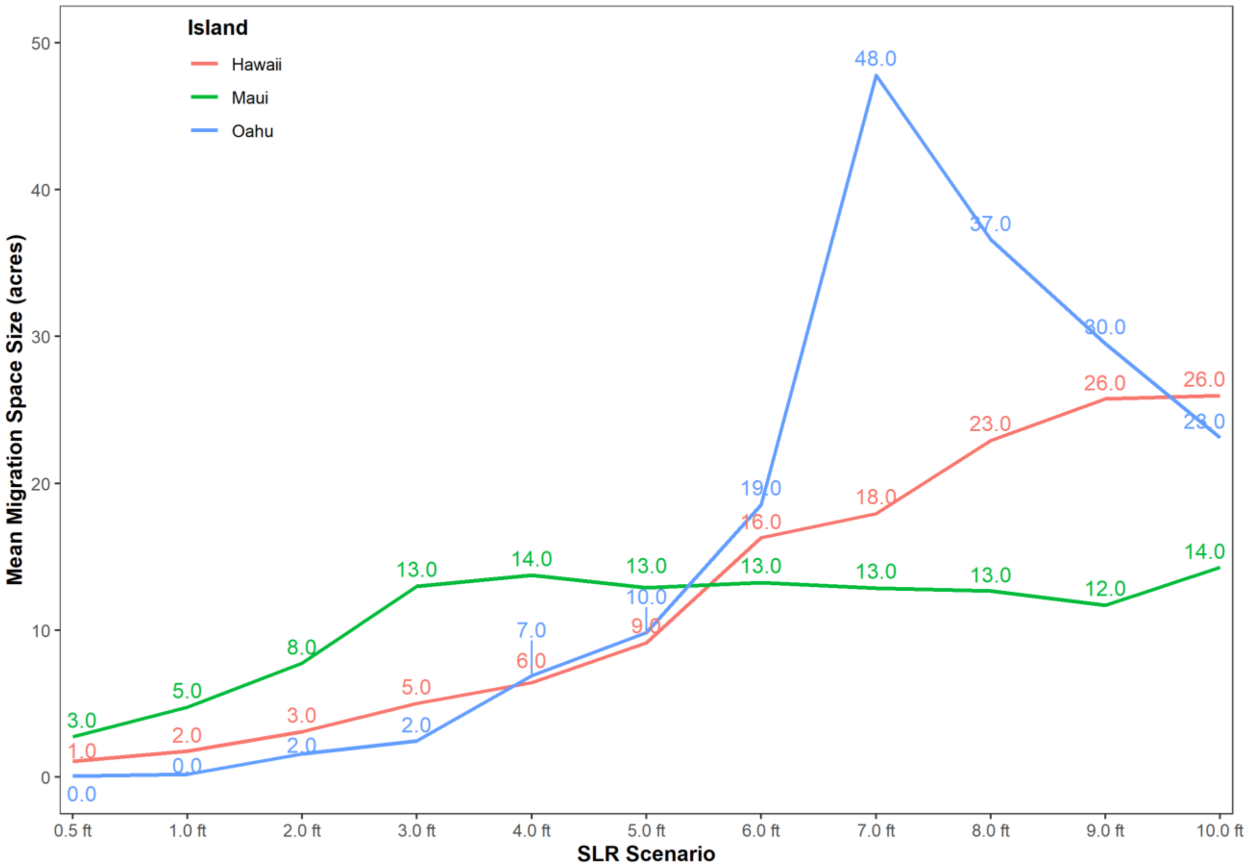

CHAPTER 6

DISCUSSION

In this study, we estimated the relative resilience of tidal marsh and unconsolidated shore sites based on the amount and configuration of each site's migration space. The results identify the places that could potentially retain species and ecological functions under rising sea levels because they have the space needed to allow the tidal complex to migrate and access to that space is not blocked by development. Sites that ranked high for resilience had relatively large areas of migration space and easily-accessed migration space. These sites offer more options for rearrangement and continued productivity than sites that lack these characteristics, and we hypothesize that they will be relatively more resilient to sea level rise. Although there is ample and accumulating evidence demonstrating that these conditions can lead to migration of the tidal complex and the development of new coastal habitats, we do not know for certain that this will occur, nor do we know the specifics of how each site will adapt and transform.

A recent study of long-term trends in a Gulf of Mexico tidal marsh found that at a regional scale, tidal marsh migration was able to outpace sea level rise. In the Big Bend area of Florida's Gulf Coast, Raabe and Stumpf (2016) compared nineteenth century topographic sheets with satellite imagery and found marsh migration led to a net gain of 25,946 acres (105 km^2) of marsh, a 23% increase over a 120-year period during which the study region experienced increased tidal amplitude and an average SLR rate of 1.5 mm/year. While 10,626 acres (43 km^2) of tidal marsh were lost to open water at the shoreline, the expansion of tidal habitats into adjacent forested lowlands offset this loss by a factor of three. The authors conclude that despite low sediment inputs and increasing sea levels, this region's coastal marshes were able to expand because they exist in a relatively undeveloped landscape with limited hydrologic modifications and have access to a large and intact migration space. The authors also note some additional characteristics that may have increased marsh resilience, including a low-energy environment and an underlying karst substrate that is less prone to erosion than unconsolidated sediments.

Another recent analysis examined tidal wetland changes in the Chesapeake Bay region of the US, an area experiencing some of the highest relative SLR rates in the world (Schieder et al., 2018). The results showed that since the late 1800s, the study region experienced a small net gain of 1,700 acres (7 km^2) of marsh, a 2% increase, due primarily to marsh migration into adjacent lowlands. While there was a net gain across the region, marsh changes were quite variable by map unit (individual topographic sheet). For example, in the Cape Charles, Virginia map unit, roughly 90% of marshes were lost, but the Potomac River, Maryland map unit saw a 400% increase in marsh area. In addition, some areas, such as the Blackwater River, had low quality topographic sheets and were unable to be examined in the analysis. Using projections for the entire region, the authors conclude that roughly 100,000 acres (400 km^2) of new marsh have been created from the drowning of adjacent uplands since the late 1800s. Marsh migration rates were weakly correlated with slope and development of the adjacent migration space, suggesting other processes also likely contributed to this expansion.

A look at the Blackwater National Wildlife Refuge, a well-studied site within the Chesapeake Bay region, shows how local site-specific conditions and management can impact marsh migration. Tide gauges in this region show that sea level has risen by over a foot since 1938, and analysis of aerial photos documented a corresponding loss of 5,028 acres (20 km^2) of tidal marsh in the refuge over the subsequent 68-year period (Lerner et al., 2013). During the same period, the refuge gained 2,949 acres (12 km^2) of new marsh through upslope migration of tidal marsh into the migration space that became available as sea levels rose. Although these observations confirm that the tidal complex is migrating and new tidal marsh is forming, the concern is that the emerging area of new marsh is not keeping pace with losses of existing marsh and could result in a net loss of both marsh habitat and associated saltmarsh-dependent birds.

Marsh loss in the Blackwater NWR was primarily due to inundation, but it was exacerbated by nutria (*Myocastor coypus*), a large semi-aquatic rodent that consumes vegetation and creates erosion-promoting channels (Lerner et al., 2013). Similarly, in South Carolina, vegetation-feeding periwinkle snails (*Littorina littorea*) have been found to transform healthy marsh to mudflats in a matter of months under a regime of increased inundation, and the consequent lack of snail predators such as blue crabs and turtles. Increased periwinkle feeding may be a factor in salt marsh loss from South Carolina to Texas since 2000 (Brown University, 2005). Managers emphasize that at Blackwater, strategies aimed at facilitating marsh migration had to be complemented by strategies to slow marsh loss such as managing herbivores and/or spreading thin layer sediment across the marsh surface. A recent study of marsh bird occupancy at the forest-marsh interface of tidal marshes in the Albemarle-Pamlico Peninsula of North Carolina highlights the potential of prescribed fire as a strategy to facilitate marsh migration (Taillie & Moorman, 2019). Fire appeared to increase bird diversity as the authors found that the occupancy of clapper/king rail (*Rallus crepitans/elegans*) was greater at sites that had experienced high fire frequency in the past decade, and the occupancy of all focal taxa was higher in areas that had vegetation characteristics consistent with fire effects, including lower density of herbaceous plants and shorter woody vegetation.

One method of potentially slowing wetland loss is to artificially supply sediments to subsiding marshes. Known as thin-layer sediment application, this method aims to help subsiding marshes accrete sediment by spraying a sediment slurry under high pressure over the marsh surface. The technique was developed in Louisiana, which leads the United States in coastal wetland loss, and has since been applied at many sites on the Gulf and Atlantic coasts. The ability of this approach to prevent loss appears uncertain, but some studies show promising short-term results (Ray, 2007). A two-year study on Masonboro Island in North Carolina (Leonard et al., 2002; Croft et al., 2006) found that deteriorated marsh plots increased their elevation by 8.5 cm after sediment treatments, while treated reference plots increased by 10 cm. They found a corresponding increase in the mean stem density of *Spartina sp.* across all plots. In Venice Louisiana, sites that received moderate amounts of dredged material (5-12 cm) still had better vegetative growth and soil conditions than reference marshes seven years after the treatment (Mendelssohn & Kuhn, 2003). Other studies in Georgia (Reimold et al., 1978) and Louisiana (Cahoon & Cowan, 1987; LaSalle, 1992) have indicated that response is sensitive to depth of deposition, slope of the marsh surface, wave action, timing of storm events, and time since application. A recent global study assessing the ability of coastal wetlands to build up vertically by sediment accretion or laterally by migration, found that the resilience of global wetlands is primarily driven by the availability and accessibility of migration space (Schuerch et al., 2018). Collectively, the studies suggest that thin layer sediment applications are unlikely to offset the persistent long-term effects of sea level rise but may be useful in alleviating short-term marsh losses or in facilitating the migration of marshes into their migration space. Accordingly, the Tampa Bay Regional Council, in conjunction with EA Engineering, has suggested that an initial target site for thin-layer spreading be areas where marsh migration is not possible (EA Engineering, 2018).

Our results are based on site level attributes that could be mapped consistently at a regional scale. This approach allows for accurate comparisons among sites but can limit the utility of the dataset in making fine-scale, within-site decisions. We recommend the study be used as a screening tool for exploring the region, making decisions among sites, and grasping the magnitude and spatial distribution of the SLR challenge. The data sets that underlie this study all have a degree of error even though they were reviewed by our team. Once a planner decides where to work, local data and field surveys will be necessary before proceeding.

Our goal was to make this study as objective and transparent as possible, but subjectivity was inevitably introduced into the analysis at several points. Foremost among these was the relative weighting of individual resilience factors with respect to their influence on resilience.

Going forward, we plan to integrate the results of this study with our terrestrial resilience map and web tools (Anderson et al., 2022). The terrestrial study identified climate resilient sites for land conservation, but did not address the coastal zone, which was masked-out on the final maps. Both studies were designed to help users make informed decisions when facing large uncertainties about climate and SLR. However, they are not intended to replace basic conservation principles such as the importance of coastal reserves, reducing direct threats, managing land appropriately, and using natural resources in a sustainable way.

We expect the coastal sites to change dramatically over the next century with our familiar tidal marsh and tidal flats migrating onto the adjacent lowlands and much of the existing marsh converting to open water. Identifying those places where conservation actions could succeed and managing those sites to adapt to change is a first step in sustaining the diversity and natural services of our coastal systems. Further, the results from this study can be used to identify potential sites for restoration, defined as sites that have the physical characteristics needed to accommodate marsh migration, but the migration space is largely inaccessible due to roads or other development. We hope that this study and the accompanying tools prove useful to planners and conservationists in identifying where to focus conservation action, and potential strategies to employ.

REFERENCES

Anderson, M.G., A. Barnett, M. M. Clark, S. Gon, A. Olivero, J. Prince, and S. Tom. 2022. Resilient Sites and Connected Landscapes for Terrestrial Conservation in Hawaii. The Nature Conservancy, Center for Resilient Conservation Science.

Anderson, M.G. and Barnett, A. 2019a. Resilient Coastal Sites for Conservation in the South Atlantic US. The Nature Conservancy, Eastern Conservation Science.

Anderson, M.G. and Barnett, A. 2019b. Resilient Coastal Sites for Conservation in the Gulf of Mexico US. The Nature Conservancy, Eastern Conservation Science.

Anderson, M.G., Barnett, A., Clark, M., Prince, J., Olivero Sheldon, A., & Vickery, B. 2016. Resilient and Connected Landscapes for Terrestrial Conservation. The Nature Conservancy, Eastern Conservation Science, Eastern Regional Office. Boston, MA.

Anderson, M.G., Clark, M., & Olivero Sheldon, A. 2014. Estimating Climate Resilience for Conservation across Geophysical Settings. *Conservation Biology* 28 (4): 959–970, DOI: 10.1111/cobi.12272

Anderson, M.G., & Ferree, C.E. 2010. Conserving the Stage: climate change and the geophysical underpinnings of species diversity. *PLoSONE* July 5: 7 e11554. http://dx.plos.org/10.1371/journal.pone.0011554

Beier, P., Hunter, M.L., & Anderson, M.G. 2015. Special Section: Conserving Nature's Stage. *Conservation Biology* 29 (3): 1523-1739. http://dx.doi.org/10.1111/cobi.12511.

Brown University. 2005. "Surprising Killer of Southeastern Salt Marshes: Common Sea Snails." *ScienceDaily*. ScienceDaily, 20 December 2005.

Cahoon, D. R., & Cowan Jr., J.H. 1987. Spray disposal of dredged material in coastal Louisiana: Habitat impacts and regulatory policy implications. Louisiana Sea Grant College Program. Baton Rouge, LA: Center for Wetlands Resources, Louisiana State University.

Chaffee, C. 2017. Coastal policy analyst for the Rhode Island Coastal Resources Management Council. personal communication. April 4, 2017.

Croft, A. L., Leonard, L.A., Alphin, T., Cahoon, L.B., & Posey, M. 2006. The effects of thin layer sand renourishment on tidal marsh processes: Masonboro Island, North Carolina. *Estuaries and Coasts* 29:737-750.

DeConto, R. M., & Pollard, D. 2016. Contribution of Antarctica to past and future sea-level rise. *Nature 531*(7596): 591-597. https://doi.org/10.1038/nature17145

Donnelly, J.P., & Bertness, M.D. 2001. Rapid shoreward encroachment of salt marsh cordgrass in response to accelerated sea-level rise. PNAS 98 (25): 14218-23. www.pnas.org/cgi/doi/10.1073/pnas.251209298

EA Engineering and Science. 2018. Thin Layer Sediment Placement – Improving Habitat and Coastal Resilience. Unpublished presentation and recommendations.

Ganju, N.K., Defne, Z., Kirwan, M.L., Fagherazzi, S., D'Alpaos, A., & Carniello, L. 2017. Spatially integrative metrics reveal hidden vulnerability of microtidal salt marshes. *Nature Communications* 8:14156. DOI: 10.1038/ncomms14156

Gill, J. L., Blois, J. L., Benito, B., Dobrowski, S., Hunter, M. L. & McGuire, J. L. 2015. A 2.5-million-year perspective on coarse-filter strategies for conserving nature's stage. *Conservation Biology* 29: 640–648. doi:10.1111/cobi.12504

Ecoregional Planning Team, The Nature Conservancy Hawai`i. 2006. An Ecoregional Assessment of Biodiversity Conservation for the Hawaiian High Islands. http://www.hawaiiecoregionplan.info/home.html

Herold, N. 2020. NOAA Sea Level Rise (SLR) Viewer marsh migration data (2.4-m), with no accretion rate, for all SLR scenarios from 0.5-ft. to 10.0-ft. for Hawai'i. Personal communication March 24, 2020.

Hill, B.R. 1996. Hawaii wetland resources. p. 167–172. In J. D. Fretwell, J. S. Williams, and P. J. Redman (compilers) National Water Summary on Wetland Resources. U.S. Geological Survey, Reston, VA, USA. Water-Supply Paper 2425.

IPCC. 2013. Summary for Policymakers. In: Climate Change 2013: The Physical Science Basis. Contribution of Working Group I to the Fifth Assessment Report of the Intergovernmental Panel on Climate Change [Stocker, T.F., D. Qin, G.-K. Plattner, M. Tignor, S.K. Allen, J. Boschung, A. Nauels, Y. Xia, V. Bex and P.M. Midgley (eds.)]. Cambridge University Press, Cambridge, United Kingdom and New York, NY, USA.
Johnson, Z., Leibowitz, S., & Hill, R. 2019. Revising the index of watershed integrity national maps. *Science of the Total Environment.* 651:2615-2630. https://doi.org/10.1016/j.scitotenv.2018.10.112

LaSalle, M.W. 1992. Effects of thin-layer disposal of dredged material in Louisiana coastal marshes (Unpublished report). Vicksburg, MS: U.S. Army Engineer Waterways Experiment Station.

Lawler J.J, Ackerly, D.D., Albano, C.M., Anderson, M.G., Dobrowski, S.Z., Gill, J.L., Heller, N.E., Pressey, R.L., Sanderson, E.W., & Weiss, S. B. 2015. The theory behind, and challenges of, conserving nature's stage in a time of rapid change. *Conservation Biology* 29: 618–629.

Leonard, L., Posey, M., Cahoon, L., Laws, R., & Alphin, T. 2002. Sediment recycling: Marsh nourishment through dredged material disposal. Final Report to NOAA/UNH Cooperative Institute for Coastal and Estuarine, Environmental Technology (CICEET). http://people.uncw.edu/lynnl/Ciceetfinalreport.pdf

Lerner, J.A., Curson, D.R., Whitbeck, M. & Meyers, E.J. 2013. Blackwater 2100: A strategy for salt marsh persistence in an era of climate change. The Conservation Fund (Arlington, VA) and Audubon MD-DC (Baltimore, MD).

Lucey, K. New Hampshire Coastal Program. Personal Communication. April 4, 2017.

Macdonald, G.A., Abbott, A.T., and Peterson, F. L., 1970, Volcanoes in the sea-The geology of Hawaii: Honolulu, University of Hawaii Press. 517 p.

Maine Natural Areas Program. 2016. Coastal Resiliency Datasets, Schlawin, J. & Puryear, K., project leads. http://www.maine.gov/dacf/mnap/assistance/coastal_resiliency.html

Marcy, D., Herold, N., Waters, K., Brooks, W., Hadley, B., Pendleton, M., Schmid, K., Sutherland, M., Dragonov, K., McCombs, J., Ryan, S. 2011. New Mapping Tool and Techniques for Visualizing Sea Level Rise and Coastal Flooding Impacts. National Oceanic and Atmospheric Administration (NOAA) Coastal Services Center. Originally published in the Proceedings of the 2011 Solutions to Coastal Disasters Conference, American Society of Civil Engineers (ASCE), and reprinted with permission of ASCE (https://coast.noaa.gov/slr/).

Mendelssohn, I., & Kuhn, N.L. 2003. Sediment subsidy: effects on soil-plant responses in a rapidly submerging coastal salt marsh. *Ecological Engineering* 21:115-128.

National Oceanic and Atmospheric Administration (NOAA). 2020a. Office for Coastal Management. "C-CAP Land Cover, Big Island, Hawaii from 2010-06-15 to 2010-08-15," "C-CAP Land Cover, Kauai, Hawaii from 2010-06-15 to 2010-08-15," "C-CAP Land Cover Lanai, Hawaii from 2010-06-15 to 2010-08-15," "C-CAP Land Cover, Maui, Hawaii from 2010-06-15 to 2010-08-15," "C-CAP Land Cover, Molokai, Hawaii, from 2010-06-15 to 2010-08-15," "2011 C-CAP Land Cover of Oahu, Hawaii from 2010-06-15." Coastal Change Analysis Program (C-CAP) Regional Land Cover. Charleston, SC: NOAA Office for Coastal Management. Accessed May 2020 at www.coast.noaa.gov/ccapftp.

National Oceanic and Atmospheric Administration (NOAA). 2020b. NOAA Office for Coastal Management Sea Level Rise Data: 1-10 ft. Sea Level Rise Inundation Extent. Accessed Sept. 2020 at https://www.fisheries.noaa.gov/inport/item/48106.

Ngu, Ash. "Hawaii's Beaches Are Disappearing." *ProPublica*, ProPublica, 29 Dec. 2020, https://projects.propublica.org/hawaii-beach-loss/.

Perlwitz, J., T. Knutson, J.P. Kossin, and A.N. LeGrande. 2017. Large-Scale Circulation and Climate Variability. *Climate Science Special Report: Fourth National Climate Assessment*, Volume I. Wuebbles, D.J., D.W., Fahey, K.A. Hibbard, D.J. Dokken, B.C. Stewart, and T.K. Maycock, Eds., U.S. Global Change Research Program, Washington, DC, USA, 161-184.

Raabe, E.A. & Stumpf, R.P. 2016. Expansion of Tidal Marsh in Response to Sea Level Rise: Gulf Coast of Florida, USA. Estuaries and Coasts 39 (1): 145-157, DOI: 10.1007/s12237-015-9974-y.

Rahmstorf, S., Cazenave, A., Church, J.A., Hansen, J.E., Keeling, R.F., Parker, D.E., & Somerville, R.C.J. 2007: Recent climate observations compared to projections. *Science* 316: 709, doi:10.1126/science.1136843.

Raposa, K.B., Wasson, K., Smith, E., Crooks, J.A., Delgado, P., Fernald, S.H., Ferner, M.C., Helms, A., Hice, L.A., Mora, J.W., Puckett, B., Sanger, D., Shull, S., Spurrier, L., Stevens, R., & Lerberg, S. 2016. Assessing tidal marsh resilience to sea-level rise at broad geographic scales with multi-metric indices. *Biological Conservation* 204 (Part B): 263-275, http://dx.doi.org/10.1016/j.biocon.2016.10.015

Ray, G. L. 2007. Thin layer disposal of dredged material on marshes: A review of the technical and scientific literature. ERDC/EL Technical Notes Collection (ERDC/EL TN-07-1), Vicksburg, MS: U.S. Army Engineer Research and Development Center.

Reimold, R. J., Hardisky, M.A., & Adams, P.C. 1978. The effects of smothering a *Spartina alterniflora* salt marsh with dredged material. Dredged Material Research Program Technical Report D-78-38. Vicksburg, MS: U.S. Army Engineer Waterways Experiment Station.

Schieder, N.W., Walters, D.C., & Kirwan, M.L. Massive Upland to Wetland Conversion Compensated for Historical Marsh Loss in Chesapeake Bay, USA. 2018. *Estuaries and Coasts* 41: 940. https://doi.org/10.1007/s12237-017-0336-9

Schuerch, M., Spencer, T., Temmerman, S., Kirwan, M L., Wolff, C., Linck, D., McOwen, C.J., Pickering, M.D., Reef, R., Vafeidis, A.T., Hinkel J., Nicholls, R.J., & Brown, S. 2018. Future response of global coastal wetlands to sea-level rise. *Nature* 561: 231-234.

Sharp, R., Tallis, H.T., Ricketts, T., Guerry, A.D., Wood, S.A., Chaplin-Kramer, R., Nelson, E., Ennaanay, D., Wolny, S., Olwero, N., Vigerstol, K., Pennington, D., Mendoza, G., Aukema, J., Foster, J., Forrest, J., Cameron, D., Arkema, K., Lonsdorf, E., Kennedy, C., Verutes, G., Kim, C.K., Guannel, G., Papenfus, M., Toft, J., Marsik, M., Bernhardt, J., Griffin, R., Glowinski, K., Chaumont, N., Perelman, A., Lacayo, M. Mandle, L., Hamel, P., Vogl, A.L., Rogers, L., Bierbower, W., Denu, D., & Douglass, J. 2016. InVEST +VERSION+ User's Guide. The Natural Capital Project, Stanford University, University of Minnesota, The Nature Conservancy, and World Wildlife Fund.

Slangen, A.B.A., M. Carson, C.A. Katsman, R.S.W. van de Wal, A. Kohl, L.L.A. Vermeersen, and D. Stammer. 2014. Projecting twenty-first century regional sea-level changes. Climatic Change, 124 (1), 317-332.

Snedden, G.A., Cretini, K., & Patton, B. 2015. Inundation and salinity impacts to above- and belowground productivity in Spartina patens and Spartina alterniflora in the Mississippi River deltaic plain: Implications for using river diversions as restoration tools. *Ecological Engineering*: 81 (8): 133–139.

"Rising Sea Level." Climate Change Portal, State of Hawaii, January 6, 2022, https://climate.hawaii.gov/hi-facts/sea-level-rise/

Sweet, W.V., Dusek, G., Obeysekera, J., & Marra, J. 2018. Patterns and Projections of High Tide Flooding Along the U.S. Coastline using a Common Impact Threshold. NOAA Technical Report NOS COOPS 86.
https://tidesandcurrents.noaa.gov/publications/techrpt86_PaP_of_HTFlooding.pdf

Sweet, W.V., Kopp, R.E., Weaver, C., Obeysekera, J., Horton, R., Thieler, E.R. & Zervas, C. 2017. Global and Regional Sea Level Rise Scenarios for the United States. NOAA Technical Report NOS COOPS 83.
tidesandcurrents.noaa.gov/publications/techrpt83_Global_and_Regional_SLR_Scenarios_for_the_US_fin al.pdf

Taillie, P. J., & Moorman, C.E. 2019. Marsh bird occupancy along the shoreline-to-forest gradient as marshes migrate from rising sea level. *Ecosphere* 10 (1): e02555. 10.1002/ecs2.2555

Thieler, E.R., & Hammar-Klose, E.S. 1999. National Assessment of Coastal Vulnerability to Future Sea-Level Rise: Preliminary Results for the U.S. Atlantic Coast. U.S. Geological Survey, Open-File Report 99-593.

APPENDIX

I

SCORING METHODS

Z-scores

In order to identify resilient and vulnerable coastal sites on each of the six Hawaiian Islands, we transformed each metric to standardized normalized scores (z-scores) so that each had a mean of zero and a standard deviation of one. A z-score is calculated using the following formula:

$$z = (X - \mu) / \sigma$$

where z is the z-score, X is the value of the attribute, μ is the mean of the attribute for all sites on the island, and σ is the standard deviation of the attribute for all sites on the island. The resultant z-score indicates how many standard deviations a particular site is from the island mean for a variable. For example, a site with a z-score of 1 indicates that the value for this attribute is 1 standard deviation greater than the attribute mean of all sites on the island.

We assigned all z-scores to one of seven categories (Table Aa-1).

Table A1-1. Z-score classes with corresponding abbreviations and colors used in the report and spatial data.

Z-score Class	Figure Color	Value Range
Far Above Average (FAA)		> 2 standard deviations
Above Average (AA)		1 to 2 standard deviations
Slightly Above Average (SAA)		0.5 to 1 standard deviations
Average (A)		-0.5 to 0.5 standard deviations
Slightly Below Average (SBA)		-0.5 to -1 standard deviations
Below Average (BA)		-1 to -2 standard deviations
Far Below Average (FBA)		< -2 standard deviations